COAST GUARD

OFFICE OF
RESEARCH & DEVELOPMENT
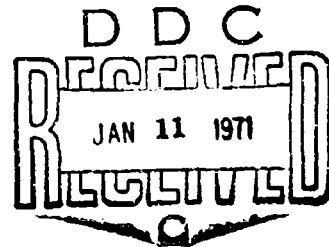CONTRACT NO. DOT-CG-03,592-A

OCEANOGRAPHIC OBSERVATIONS

AND THEORETICAL ANALYSIS OF OIL SLICKS

DURING THE CHEVRON SPILL, MARCH 1970

STEPHEN P. MURRAY
W. G. SMITH
CHOULE J. SONU

D D C

JAN 11 1971

COASTAL STUDIES INSTITUTE
LOUISIANA STATE UNIVERSITY
BATON ROUGE, LOUISIANA 70803

JULY 1970

FINAL REPORT

Prepared for: COMMANDANT (DAT)
U.S. COAST GUARD HEADQUARTERS
WASHINGTON, D.C., 20591

DATE: 4 DECEMBER 1970

This report has been submitted in fulfillment of contract DOT-CG- 03592-A
and is promulgated subject to the following qualifications:

The contents of this report reflect the views of the Coastal Studies
Institute of Louisiana State University,

which is responsible for the facts and the accuracy of the data presented
herein. The contents do not necessarily reflect the official views or
policy of the Coast Guard. This report does not constitute a standard,
specification or regulation.

J. R. IVERSEN
Captain, U. S. Coast Guard
Chief, Applied Technology Division
Office of Research and Development
U. S. Coast Guard Headquarters
Washington, D. C. 20591

Oceanographic Observations
and Theoretical Analysis of Oil Slicks
During the Chevron Spill, March 1970

Stephen P. Murray

W. G. Smith

Choule J. Sonu

Coastal Studies Institute

Louisiana State University

Baton Rouge, Louisiana 70803

July 1970

FINAL REPORT

The contents of this report reflect the views of the
Coastal Studies Institute of Louisiana State University,
which is responsible for the facts and the accuracy of
the data presented herein. The contents do not
necessarily reflect the official views or policy of the
Department of Transportation. This report does not
constitute a standard, specification or regulation.

ABSTRACT

Oceanographic obs=rvations near the Chevron spilling well off the Mississippi
Delta in March, 1970, revealed relative roles of varⁱᵒᵘˢ physical factors of the
regional estuarine system in the behavior of oil slicks. Surface stress from the
wind was most important; at speeds above 15 mph the slick orientation was generally
determined by the wind direction. The wind also indirectly affected oil which was
sunk by dispersant in that wind waves promoted mixing, which in turn affected the
vertical stability, hence eventually the velocity profile. Wind setups and setdowns
were correlated with downward and upward isopycnal movements, respectively. Both
calculations and observations showed that tidal currents produced an L-shaped slick
geometry when winds were below about 15 mph. The diurnal rotation of the tidal
currents served to limit the excursion length of oil from the source, keeping it
short of the nearest shore. The presence of fresh water from the Mississippi River
in the surface layer and the consequent development of convergence lines often
formed a natural barrier, preventing oil from encroaching upon the shore. Theo-
retical analysis using turbulent diffusion theory disclosed that the area and length
of a steady-state oil slick increased with oil discharge but decreased with the
current speed and the lateral diffusion coefficient. Slick width increased with
the rate of discharge and decreased with current speed but was independent of the
diffusion coefficient. The width/length ratio of an oil slick, which was notably
independent of current speed, was controlled only by the diffusion coefficient and
the oil discharge. In order to be able to predict oil slick behavior, understanding
of the interaction between these multiple factors is essential and, for that end,
the use of a multiple-sensor array with automatic data transfer and processing
capability is recommended.

FIGURES

iii

TABLES

▼

NOTATION

A   slick area

C   concentration; $C(y = R)$ is the concentration at the visible boundary of the slick

F   fetch

g   acceleration because of gravity; or grams

h   thickness or depth

$H_{1/3}$ significant height of waves

K   diffusion coefficient, diffusion coefficient of oil

K_o modified Bessel function of 2nd Kind and Zero Order

ℓ^* scale length or average eddy size

L   slick length

Q   rate of emission (of oil)

r   distance from the origin

$R(\xi)$ the Lagrangian autocorrelation function

t   various time parameters

T   time

U   mean horizontal current speed

U_w wind speed at 10-meter height

v' turbulent velocity in y direction

$(\overline{v'^2})^{1/2}$ intensity of turbulence, usually of oil

W   slick width

θ one-half the initial angle of dispersion of the slick, $\tan \theta = \dfrac{d\sigma}{dx} = (\overline{v'^2})^{1/2}/U$

M   millimicrons

ξ the lag time

ρ density

σ^2 the variance of particle displacements from the source

ϕ in polar coordinates, the argument

INTRODUCTION

When the Chevron production platform MP-41C caught fire and burned in February 1970, a situation was created which at the time appeared to be potentially a prelude to a disaster of major scale. Efforts to extinguish the costly fire were almost certain to lead to large losses of crude oil into the sea, and much of this seemed likely to wash ashore in various areas of the marshes on the mainland.

Figure 1 indicates the location of the accident (platform 41C); it is north and east of the Mississippi Delta and near the entrance of the Gulf outlet channel. Water depths in the general vicinity are from 20 to 50 feet. Before direct measurements were begun, a search for literature giving indications of circulation patterns in the area was made.

Scruton (1956) measured 24-hour diurnal current profiles at several stations in the Main Pass area. Two of these were in the passages into Breton Sound lying to the east and west of Breton Island. In these, ebb and flood current direction were necessarily constrained to inward and outward flow. Surface currents showed a net outward flow at the time of measurement, which was in agreement with the wind direction at the time. Another station, away from the passes and within 3 miles of the site of the 41C platform, showed more variability in flow direction but indicated even higher residual outward (in this case southeastward) flow at the surface. Scruton felt that the residual outward flow in this last case was also caused in part by the wind and by transfer of fresh water from the river out to sea at the surface. He indicated that maximum currents at times of

1
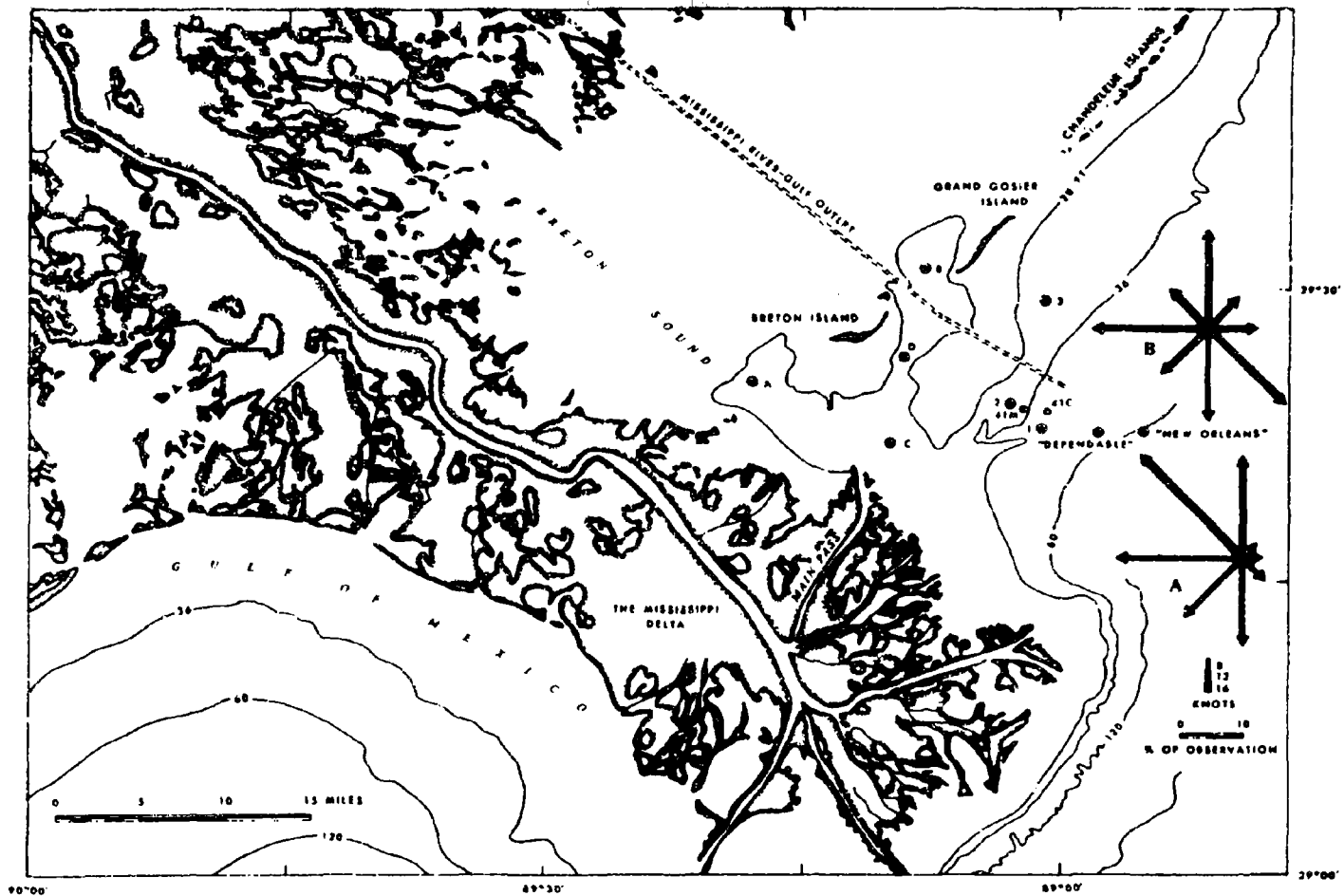
Figure 1. Location map with stations occupied in study. A is wind rose for long-term March observations. B is wind rose for March 1970 from lightship data.

tropic tides could be 1-2 knots and that at times of equatorial tides currents were much lower.

The general hydrography of the area is indicated on Figure 1 and is given in much greater detail on chart 1270 of the U.S. Coast and Geodetic Survey. An important alteration in the area since the time of Scruton's study was the dredging of the Mississippi River Gulf outlet channel to a controlled depth maintained at 36 feet, with deposition of spoil along the southwest side of the channel.

Orton (1964) gave wind data for subsquare 55 of Marsden square 81, in which the 41C platform lies. For the "average" March, on the basis of 5,331 observations, the winds are indicated on wind rose A of Figure 1. The strong northwestward and westward components seemingly would favor drift, insofar as it is wind controlled, toward the Mississippi Delta and the marshes surrounding Breton Sound. The Weather Bureau (1959) also has published data indicating that the frequency distribution of direction of wave approach for winter and spring months shows a predominance of waves coming from the east and southeast in the area of the 41C platform.

Tidal predictions given in Coast and Geodetic Survey (1970) tables for Breton Island for the month of March 1970 are shown in Figure 2.

Another very important part of the physical background necessary to an understanding of the situation is the influence of waters discharged by the Mississippi River. Figure 3 gives the stage height at New Orleans and discharge at Vicksburg, Mississippi, averaged over several years. March is typically a time of high stage and discharge, and 1970 was no exception. The discharged floodwaters are highly turbid and cool (10°C)

3
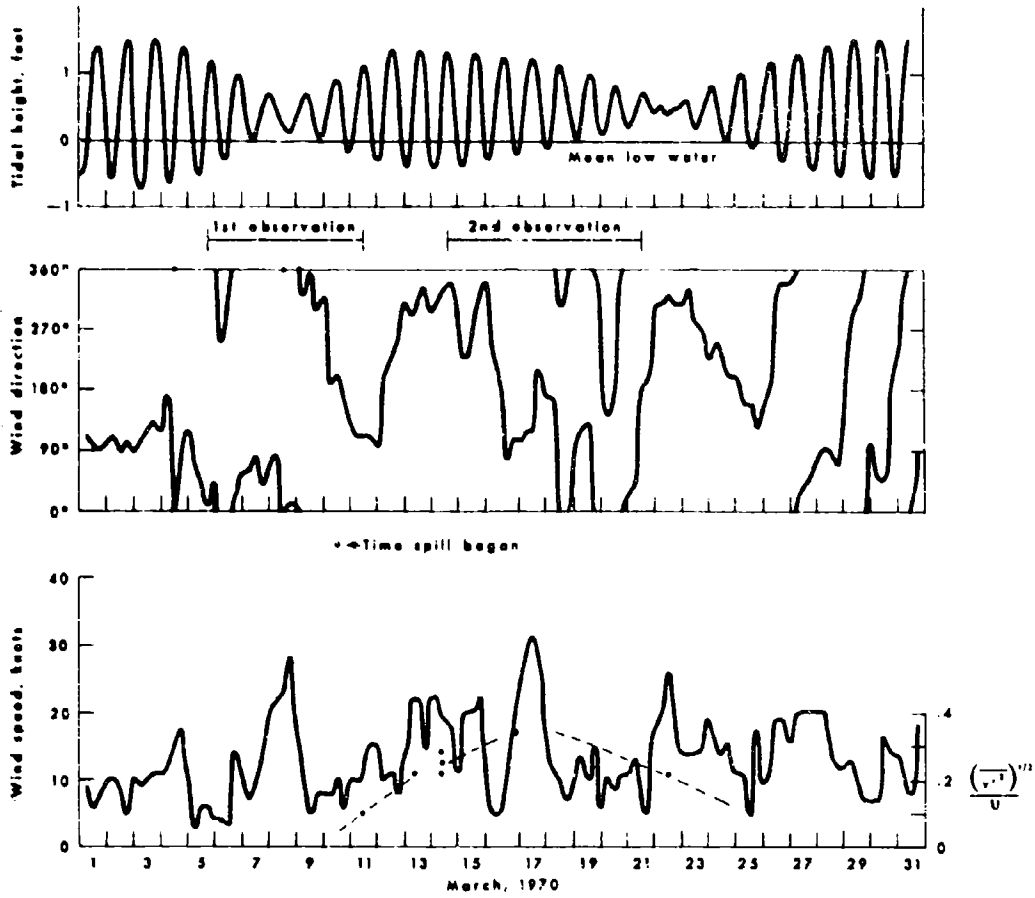
Figure 2. Tidal range for Breton Island and wind speed and direction
observed at lightship during March 1970.

4
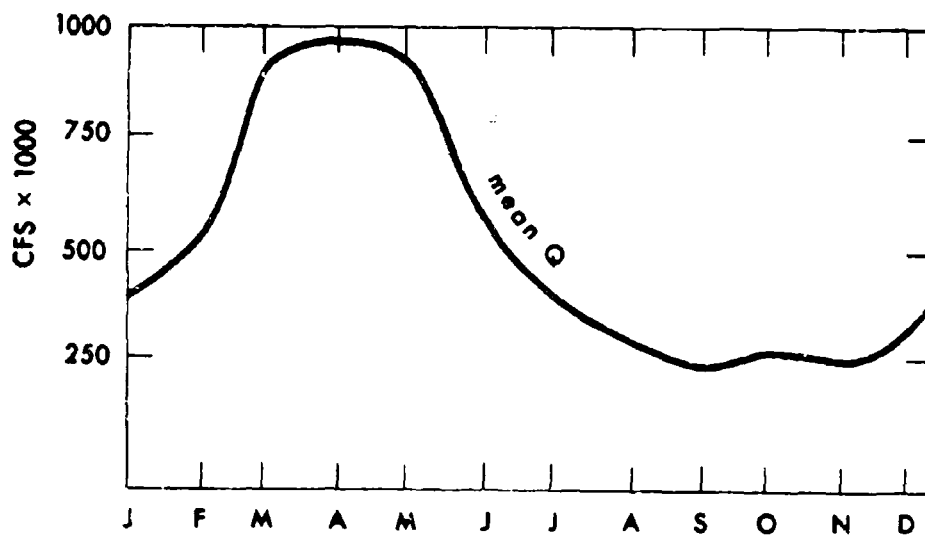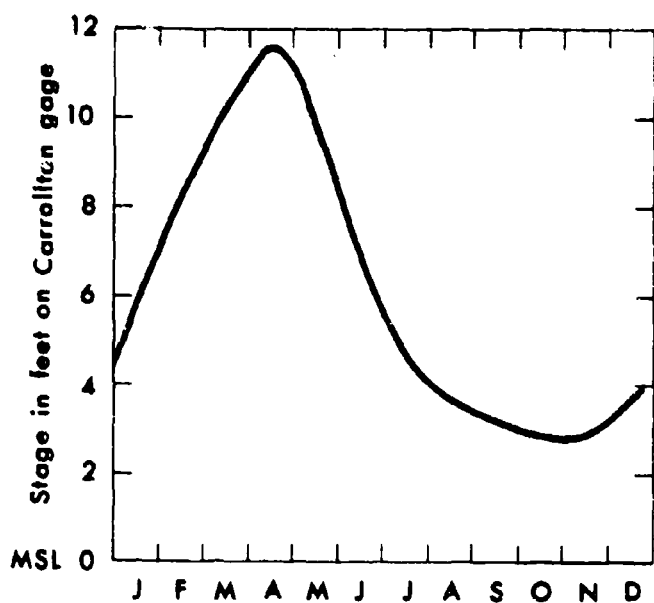
Figure 3. Stage height of Mississippi River at New Orleans and discharge at Vicksburg, long-term averages. (From F. Swaye, Ph.D. dissertation, L.S.U., 1970.)

and contrast sharply with the much less turbid and generally warmer (20°C) saline Gulf waters.

Except for the above-mentioned material, there was little background information useful for judging what might happen when oil began to spill from the Chevron platform. For this reason it was decided that, in light of the possibly dangerous situation that could develop, some basic oceanographic information should be collected before the fire was put out and during the spill. The Eighth District of the U.S. Coast Guard readily agreed to cooperate, and measurements were begun on March 5.

The most important consideration was current, particularly surface current. Temperature and salinity were found to be useful discriminators of the riverine and marine water masses which crossed the accident area. Wind records were also maintained to establish the relation these might have to surface currents. Currents at depth were monitored inasmuch as it seemed possible that a decision to use dispersants to emulsify the oil might lead to spread of oil throughout the water mass. Tides were measured directly since it was not certain how well the predicted curve would agree with the real situation. Wave height and wave period seemed useful indices that might affect diffusion of the drifting oil. Another category of observations was the direct delineation of the orientation and shape of the oil slicks in space and through time.

In all, observations were made from four different Coast Guard vessels at nine different anchorages for continuous periods ranging from 5 days to 6 hours. Slick observations were made from helicopters on a routine basis by Coast Guard personnel, usually twice a day in clear

weather. Overflights were made by several different groups using various conventional and more novel means of remote sensing to document the extent of oil slicks. These data have been made available to us by the U.S. Geological Survey and by Remote Sensing Inc., Houston, Texas. The National Aeronautics and Space Administration also made two overflights during which the C.S.I. group obtained ground truth rvations. This material has not yet been made available; however, one of us was able to inspect briefly the imagery at the Manned Spacecraft Center in Houston. A tide and wave gage was suspended from Chevron's MP-41M rig, which is about 1 mile from the damaged structure. A bottom current installation was also made at an additional site, but this instrument has not yet been recovered.

Complete records of all temperature, salinity, and current profiles made from all nine stations are presented in the appendix. Graphical records of these and other observations are presented throughout the remainder of this report.

The 41C platform caught fire at 3 a.m. on Tuesday, February 10, 1970. While it was burning unchecked most of the escaping oil, estimated by Chevron at 1,000 barrels per day, was burned and did not reach the water surface. The work near the platform necessary for quenching the fire required pumping water onto the flame, however, and this tended to wash oil into the water, resulting in light slicks for about a month before the fire was out. The first attempt (March 8) to extinguish the flame was successful, but spontaneous reignition occurred after spillage of crude oil for 6 minutes. On March 10 the fire was successfully extinguished, and oil continued to spill for approximately 1 month before all wells were capped.

7

Our observations, except for those kept and made available to us by Coast Guard personnel, were confined to two periods, March 5-11 and March 14-20.

MEASUREMENT TECHNIQUES

Tides

Tides were recorded by a Hydro Products 521 model submerged wave and tide gage. This hydrostatic pressure-sensing unit is designed for bottom installation, but since there was little time to dive to emplace the instrument properly, it was simply suspended by a rope from the MP-41M platform in firm contact with the bottom. The instrument functioned well and gave data which agree very well with tides predicted for Pensacola (Fig. 4).

Salinity-Temperature

Salinity and temperature were determined with a Beckman RS-5 induction salinometer. The induction electrode was mounted generally just above the current meter and raised and lowered to the various depths at which currents were monitored so that simultaneous temperature and salinity readings could be made. This instrument functioned well at all times. A few values above 37 parts per thousand are anomalous for this area of the Gulf of Mexico and probably indicate some instability in calibration or misreading of the instrument. Figure 5 is a record of salinity and temperature for the entire period of observations from the C.G.C. Dependable.

Winds

Wind speed and direction were recorded at quarter-hour intervals by the men on watch on the U.S.C.G.C. Dependable during the whole period of our observations on board that vessel. Crewmen on watch on the cutters

8
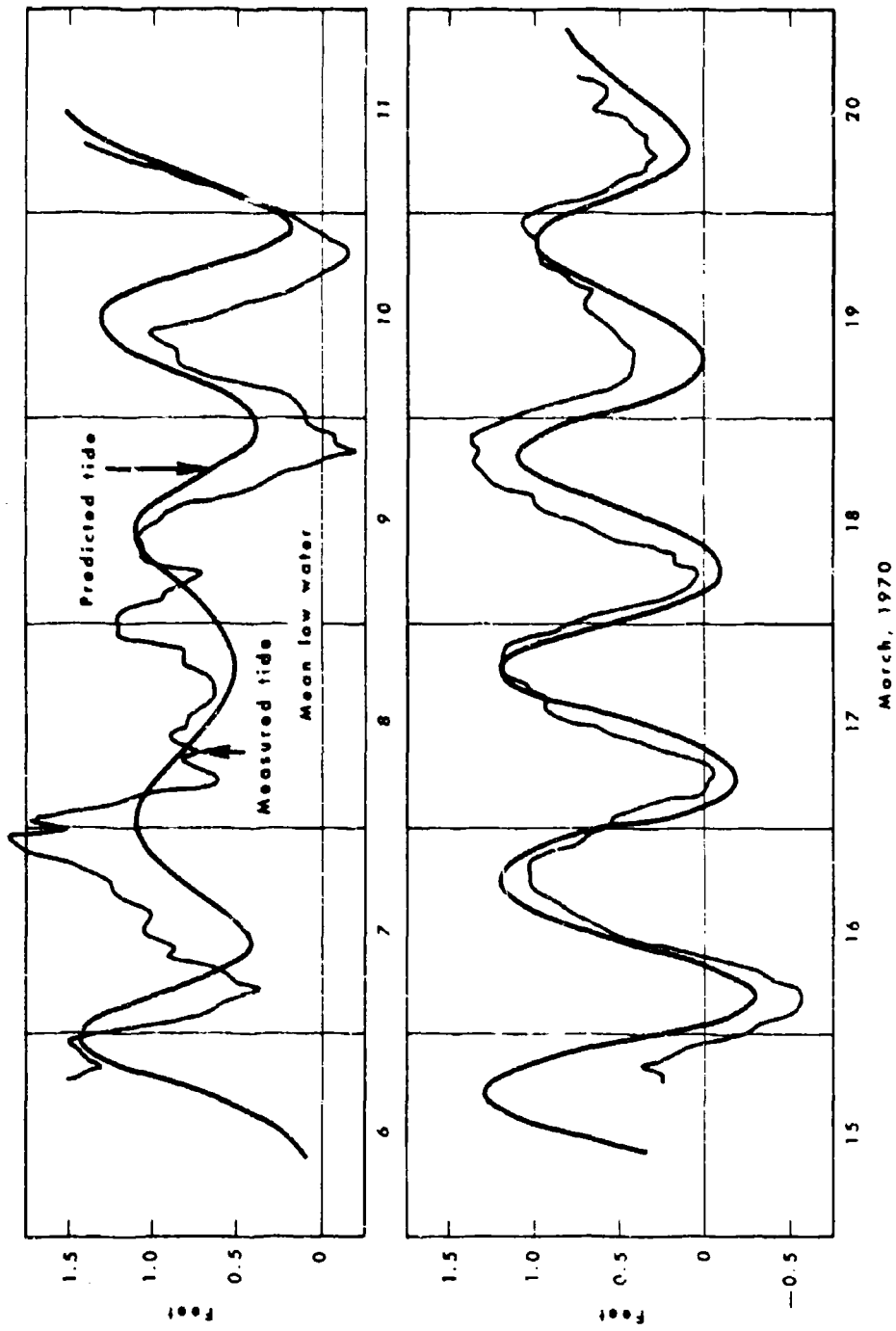
Figure 4. Observed and predicted tides.
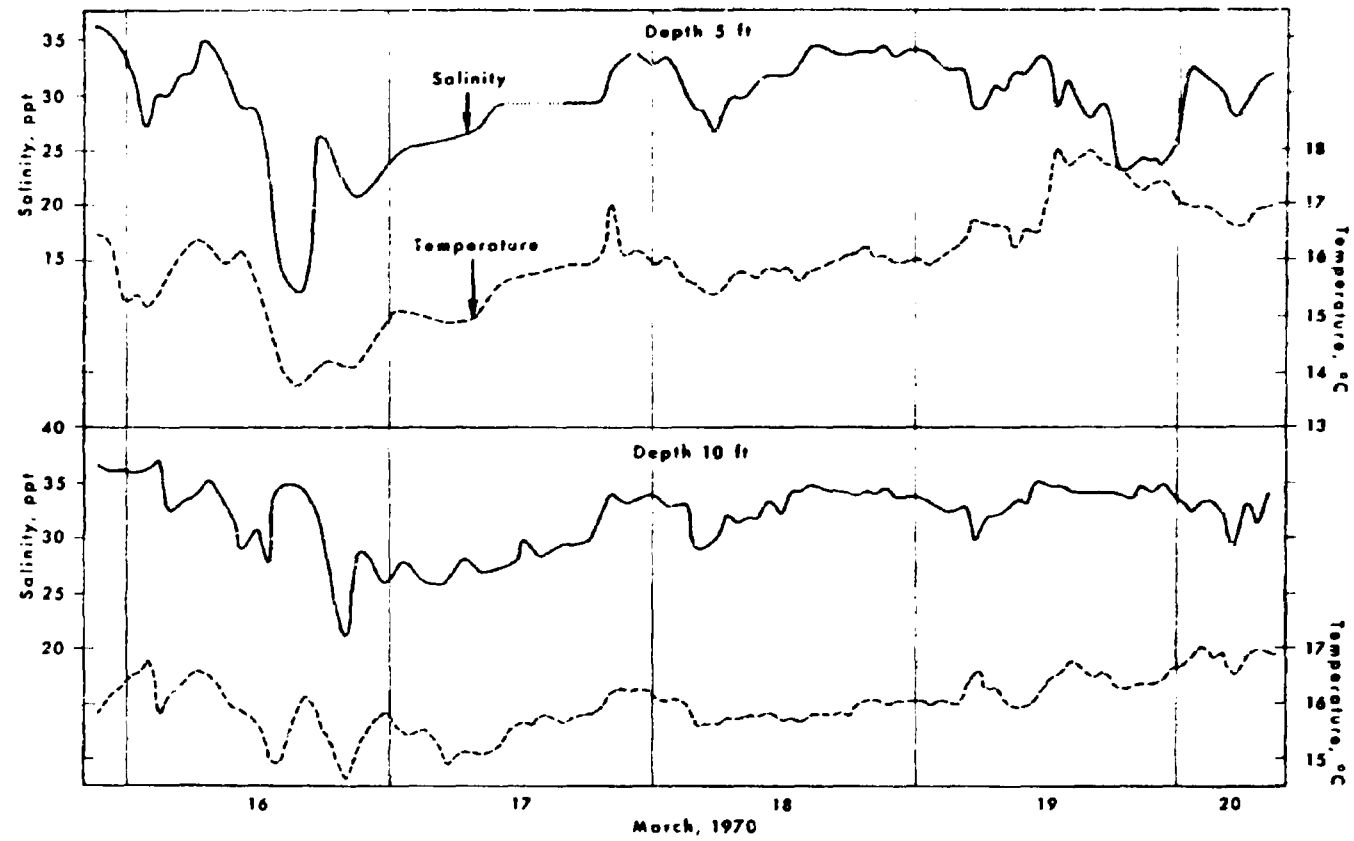
Figure 5. Salinity and temperature records from 5- and 10-foot depths at <u>Dependable</u> station.

10

<u>Pt</u>. <u>Spencer</u> and <u>Pt</u>. <u>Estero</u> also kept logs at various times of wind speed and direction at our request. The lightship <u>New Orleans</u> regularly records meteorologic data every 6 hours year-round and relays this information to the Weather Bureau. Figure 2 gives a plot of wind speed and one of wind direction for the entire month of March based on the lightship records. Figure 6 shows wind speed and direction recorded from March 15 to March 20 by the <u>Dependable</u>. On Figure 1 the lightship wind records for March are plotted as wind rose B (based on 115 observations) for direct comparison with the winds expected in an "average" March.

Currents

The most successful current monitoring was done with Marine Advisers Q-15 ducted current meters, which were raised and lowered by means of the ship's winches. Savonius rotor-type meters were employed with some success at fixed levels by suspending the instruments on cables from the cutter <u>Reliance</u> and from the lightship <u>New Orleans</u>.

The greatest difficulty in measuring currents in shallow coastal waters is the effect of the oscillatory orbital wave motions on the speed sensors. The Savonius rotor, for example, will spin up with the wave motions and can overestimate the steady current by a factor of three or four. A bidirectional ducted meter such as the Q-15, used extensively in this program, largely eliminates this error.

The chief problem in current monitoring from ships is the motion of the ship itself even when at anchor. In this study it was noted that whenever winds exceeded about 12 knots the vessels began to yaw from side to side, swinging on the anchor. This motion of the ship drags the current

11
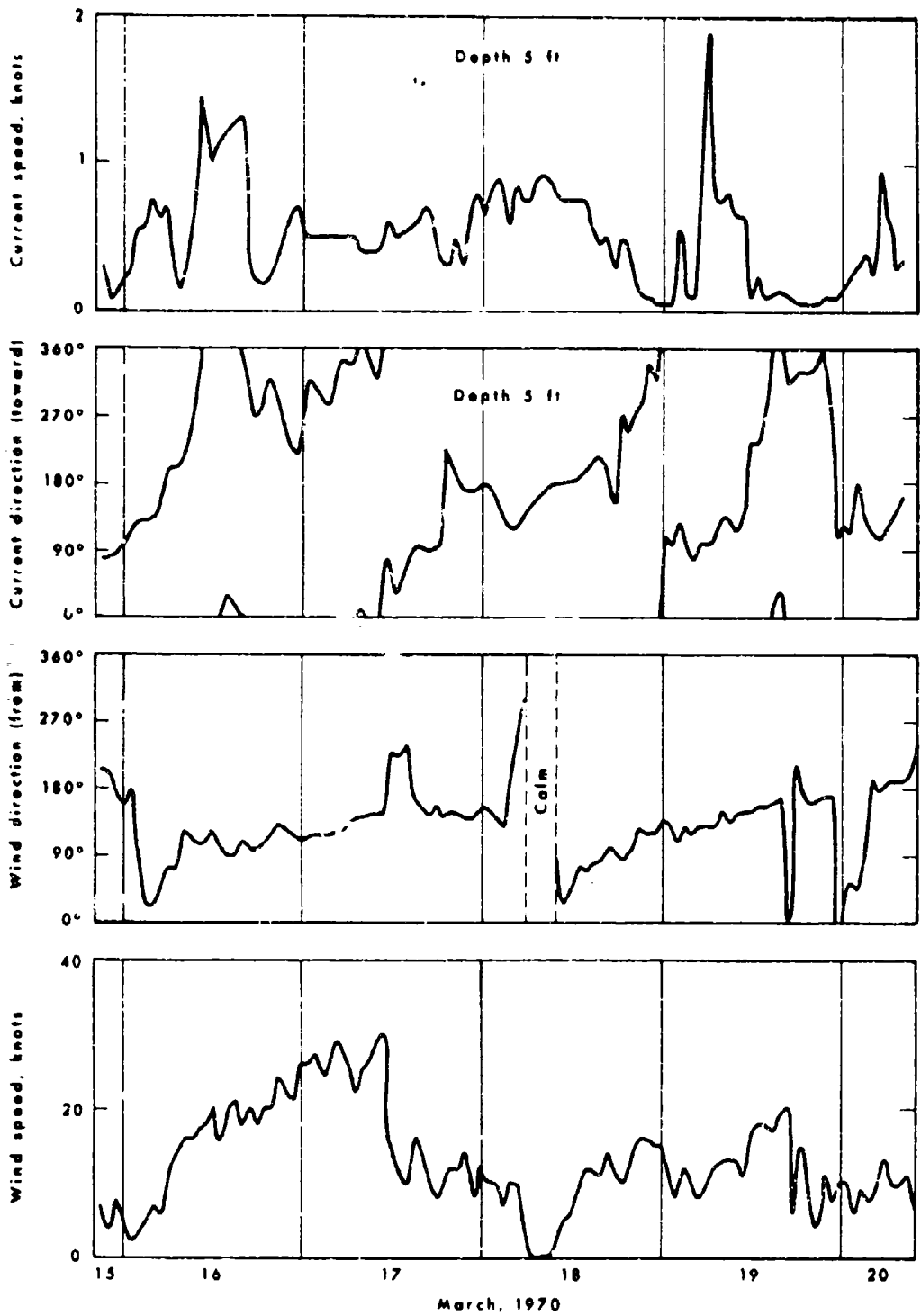
Figure 6. Current speed and direction at 5-foot depth and wind speed and direction at Dependable station.

12

meter and causes rhythmic oscillations of readout, giving errors that can be as much as .5 knot too high. This type of error is obvious on the record; all erroneous data have been deleted from consideration. Current observations from the Dependable are plotted on Figures 6 and 8.

The vertical motions of the ship are an additional problem which can give false impressions about currents. Both side-to-side swinging and vertical motion led to a generally unsatisfactory performance for the Savonius meters, and information from these is not used here. The ducted meters respond in a selective way directionally. For a detailed discussion of these types of error see Murray (1969).

Measuring currents very near to the surface with any type of suspended meter is difficult except in periods of calm sea states. The periods of high waves encountered in the study sometimes made it impossible to obtain current readings at 5 feet depth because of extreme swinging of the instrument as waves rocked the ships. Use of floating drogues or drift cards for surface current measures therefore seems preferable if adequate means of tracking are available.

Sometimes currents changed in speed very rapidly, as can be seen in Figure 6 at about 0700 CST, when current speed changed from .05 to 1.9 knots in a 2-hour period. This poses a sampling problem. The intervals for completion of a single profile were about 1 hour, meaning that readings at any given depth were repeated about once an hour. With such rapid changes taking place, this may not have been sufficient to record all peak speed periods. It would be preferable to have currents at a given depth monitored continuously.

13

Ideally, much more could have been done, and will be done as the "state of the art" for shallow-water current measuring instruments improves. It is tempting to think of moored strings of ducted current meters spaced at fixed depths and recording continuously. The moored deployment would eliminate many of the problems inherent in unsteady ships, the continuous recording would give better resolution, and the ducted instruments would give better directional response. Although this seems a greatly improved means of profiling, another approach will be necessary for continuous study of very-near-surface currents at times of varying sea state, a problem of critical importance in the movement of oil on water.

Waves

Wave height and wave period were recorded by the Hydro Products 521 model instrument previously described in the section on tides. As mentioned, this instrument was installed by suspending it from a platform. Its attachment to the platform probably added some noise to the data (particularly the wave period) owing to the effect of the structure on waves approaching from certain directions. Other than this, the records seemed excellent and are plotted in Figure 7 with wind speed for comparison.

Choppy seas are indicated by low period numbers. At 1200 CST on March 17, for instance, during a high wind, wave period reached a minimum of 3 seconds. Shortly after this the wind fell off abruptly and the record began to show a steady swell with period of about 7 seconds. The swell probably existed prior to this but was masked by the seas.

Slicks

The Coast Guard's routine Situation Reports gave direction and approximate width and length of the oil slicks when visibility conditions allowed

14
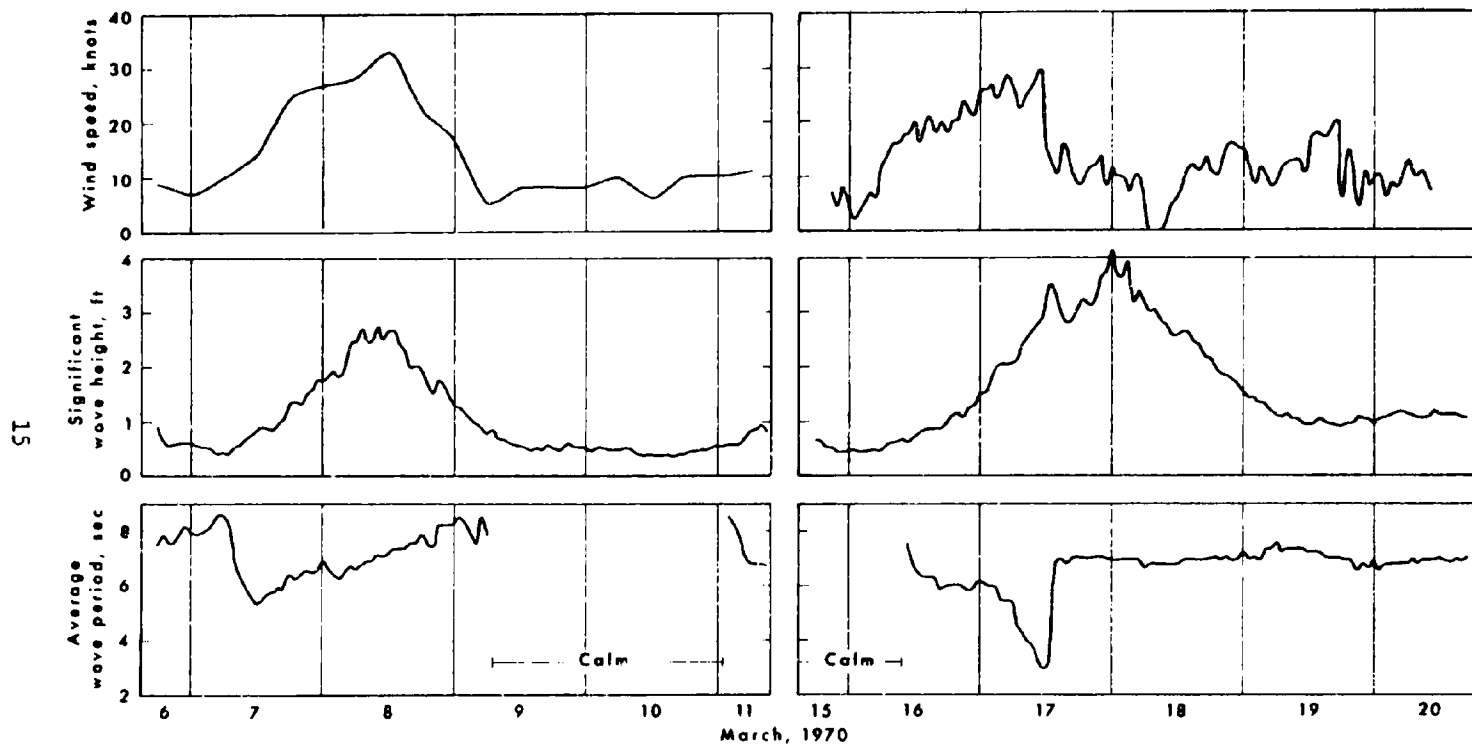
Figure 7. Wave height and wave period from 521 meter installed at Chevron platform MP-41M and wind speed for same intervals.
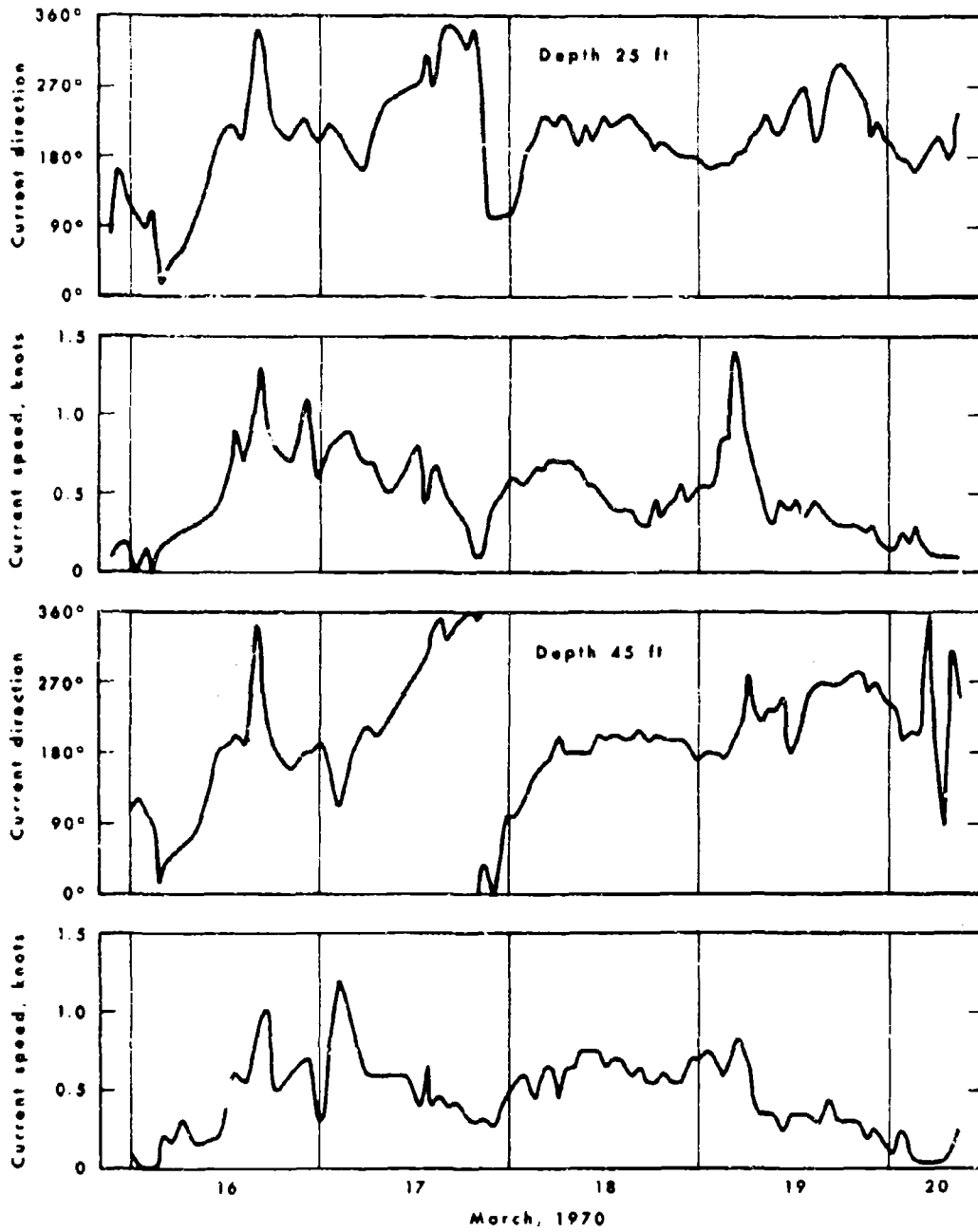
Figure 8. Current speed and direction at 25- and 45-foot depths at
<u>Dependable</u> station.

observation from helicopters or other aircraft. Aerial remote sensing by photography and infrared scanners also recorded the distribution of oil on several occasions. The infrared (8-14µ) scanning device showed the form and xtent of the oil slick especially well. In these images the lighter films of oil, which formed the greater part of the area of the slick, generally appeared darker than the surrounding water. The heavier agglomerated masses of oil, which occurred in patches up to a centimeter in thickness, showed as very light areas on the scanner imagery.

ANALYSIS AND INTERPRETATION OF DATA

During the 12 days at the site of the Chevron spill our research group collected a tremendous volume of data. This data was subsequently augmented by numerous photographs and imagery taken by several government agencies and private companies, the information in the Situation Reports, and assorted other data. Because of time limitations, in-depth analysis has been restricted to the characteristics of the currents; gross relationships between measured current, winds, and slick movements; and theoretical slick analysis. We have arranged most of the observational data in figures, and this section will be mainly a discussion of the salient features exhibited by the figures.

Tides

On Figure 2 the most conspicuous feature of the tides predicted for March is the biweekly cycle of high-range tropical tides and low-range equatorial tides, which are characteristic of this area of the Gulf of Mexico. The maximum range for tropic tides is about 2.5 feet, and the range for equatorial tides may be only 0.1 foot or less. In restricted

17

waters strong winds can increase or diminish tidal range considerably. The tides are largely of diurnal character, but semi-diurnal components may be evident, particularly during equatorial tides.

Figure 4 shows the measured tides, with predicted curves plotted for comparison. Agreement between the two is excellent, indicating that the tide predictions at Pensacola are useful for the area of study. The interval of March 6-11 spans a period of equatorial tides and that of March 15-20 covers a period transitional from tropic to equatorial. The semi-diurnal components are evident for the period of March 8-9 and again in the period March 17-20.

Salinity and Temperature

Salinity and temperature profiles in the area of the 41C platform were quite variable in the upper portions, while temperature and salinity at depths below 15 feet were rather constant at about 16°C and 35 parts per thousand, respectively. At times the temperature profiles were virtually isothermal, but a distinct halocline generally existed between 5 and 15 feet beneath the surface. During periods of high winds and waves the halocline moved downward, reflecting deeper mixing (see, for instance, the salinity records from the Dependable for March 17 cited in the appendix).

In the zone above the halocline, salinity and temperature variations at a station were extreme and sudden. Figure 9 shows the situation which existed at the Dependable just prior to and during the first NASA over-flight. A mass of highly turbid water moved past the Dependable at approximately 1330 CST, and temperatures quickly declined by 2° at the surface while salinity dropped from 24 to 13 parts per thousand. Figure 5 shows the record

18
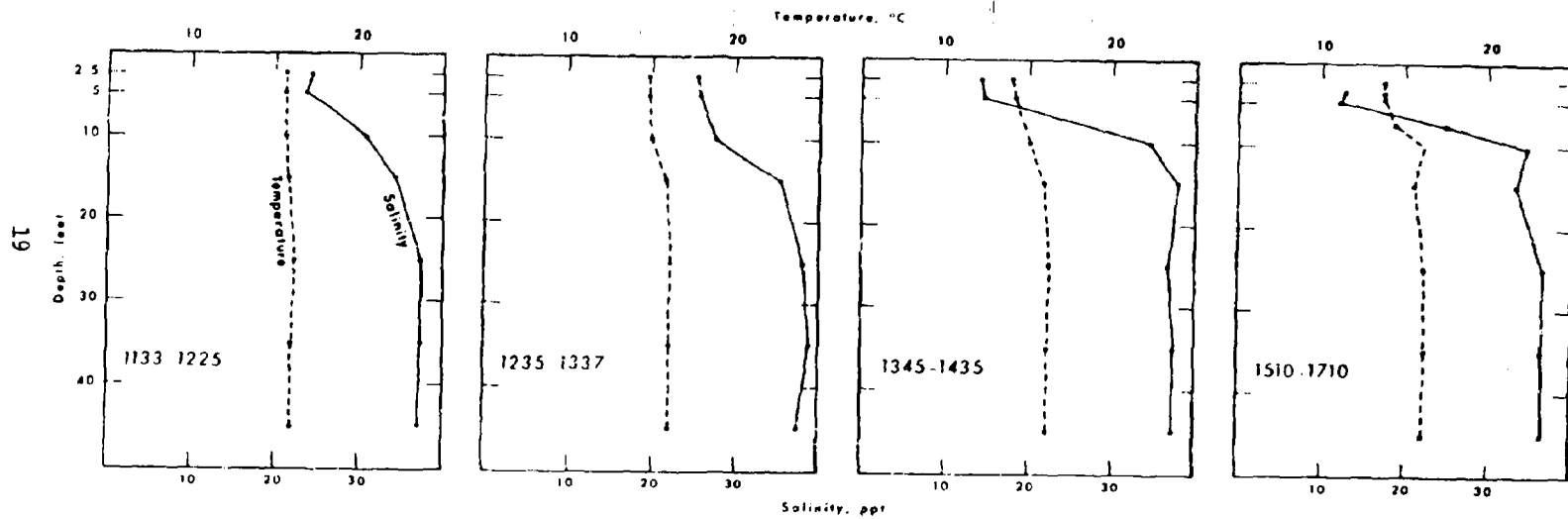
Figure 9.   Salinity and temperature profiles, <u>Dependable</u> station, March 16, 1970.

19

of this event as well as that at the 10-foot depth, where declines of temperature and salinity are not as great. A similar passage of a freshwater body was recorded in the Pt. Spencer, station 1, observations on the night of March 5, when salinities declined abruptly from 27 to 18 parts per thousand, then slowly returned to normal levels (see appendix).

These low-salinity surficial water masses usually were clearly demarcated from higher salinity waters by a sharp "tide line" or interface. Such interfaces are familiar phenomena in the Mississippi Delta area. The interface is prominent not only because of the strong contrast in turbidity across it but also because frequently there are concentrations of floating debris along it. Oil likewise tended to hang up along it. Slicks of great width would contract to narrow bands along the interface and abruptly assume the same orientation as the interface.

The fact that oil tended to be stranded along this boundary, together with the fact that only a small amount of oil reached shore from this large spill and this only on Breton and Grand Gosier islands, suggests that coastal low-salinity water masses may have acted as a buffer zone, protecting the marshlands. River water discharged from the numerous passes of the flooding Mississippi must also create a hydraulic gradient leading to a net offshore displacement of surface waters.

Winds

Wind rose B of Figure 1, based on 115 observations, shows us observed by the lightship New Orleans in March 1970. While the "average" March depicted in A shows a clear predominance of winds from the east, south, and southeast, the March 1970 record differs in the great frequency

20

of winds from the northwest. This was perhaps a fortunate circumstance in preventing spread of oil into the marshlands to the west and northwest.

The wind speeds and directions indicated in Figure 2 show the erratic nature of winds during March. The two periods of highest winds, on March 8 and March 17, occurred during the periods of observations and added variety as well as difficulty the operations. These periods are discussed in the section on waves. Average wind speed for the whole month is approximately 12 knots.

Figure 6 shows winds recorded on the Dependable for March 15-20, during most of which time winds from the southeast prevailed.

Waves

Our data on significant wave height and average wave period near 41C, displayed in Figure 7, are restricted to the periods of on-site observations, March 6-11 and March 15-20. Significant wave height $H_{1/3}$ is the average of the highest one-third of the waves. The correlative wind speed in the figure shows that each observation period had a clearly defined storm pattern. During the lightest winds the wave height diminished to 0.2-0.3 foot, while the highest waves (~4.0 feet), early on March 18, were actually swell generated offshore. The expected close correlation between wind speed and wave height is obvious, but a close examination does reveal some interesting features.

During the first storm period the wind blew from the north, a direction in which the fetch is limited to about 10 nautical miles. According to Wiegel's (1962) empirical equation, the maximum possible wave height $H_{1/3}$ is given in a nondimensional form

21

$$\frac{g\,H_{1/3}}{U_w^2} = .00305 \left(\frac{g\,F}{U_w^2}\right)^{0.466}$$

where U_w is the 10-meter wind speed and F is the fetch. This expression pre-
dicts a maximum of 4 feet for $H_{1/3}$, but the wind duration was not sufficient
to generate this height of wave; the height reached only 2.7 feet. In
addition, the fetch is too limited for any appreciable swell to develop,
and this is demonstrated by the abrupt decrease in wave height in phase with
the decay of the wind speed.

The second storm (March 16-18) blew from the southeast, the direction
of maximum fetch into this area. The wind speed attained its maximum at
1200 hours on March 17, but the maximum observed wave height of 4.2 feet
lagged by 12 hours because of the arrival of large swell from offshore.

The interaction of sea and swell is better illustrated by the wave
period diagrams in Figure 7. During the first storm, as soon as the wind
speed exceeded 10 knots tne sea began to build and the wave period dropped
abruptly to 5.3 seconds, reflecting the surface chop (wind waves), then
gradually recovered up to 8 seconds with the arrival of swell. Again, in
the second storm, the sea began to build when the wind exceeded 10 knots.
The wave period dropped gradually as low as 3 seconds until 1200 hours
March 17, when the wind speed suddenly dropped from 30 knots to 10 knots.
This discontinuity is immediately reflected in the wave period, with a
step-up in period from 3 seconds to 7 seconds as the sea quickly dissipated
and the swell predominated.

Prior studies (Johnson and Hwang, 1961; Masch, 1961) have shown that
the wave height and period can significantly affect the dispersal of fluid

22

properties such as amount of suspended solid waste or thermal maxima, and so by extension the surface oil concentration. It is unfortunate that with the excellent quality of the wave data during these two intervals there is practically no quantitative data on the oil slick with which to make comparison. The slick geometry at other times can, however, be related to the wave field indirectly through the wind speed--this is discussed in the section on diffusion theory.

Currents

A priori considerations and experience lead us to expect a mixture of current types in this area--tidal currents, wind-drift currents, slope currents from setup, setdown, and from Mississippi River outflow, and relative currents associated with freshwater-saltwater density gradients.

Near-Surface Currents.--The unreduced current speeds and directions from the 5-foot depth during March 15-20 are plotted on Figure 6, together with the wind speeds and directions. Owing mainly to exceptional logistical support, our most reliable current information comes from this period. The figure shows that the wind remained consistent from the southeastern quadrant but that the current direction rotated clockwise in three broad cycles. The periods were usually well over 24 hours; so these are not simple rotary tidal currents. The wind speed was generally greater than 10 knots and the current speed generally exceeded 0.6 knot.

A clear relationship between the wind and the 5-foot current existed during only one time interval. Between 1800 hours March 16 and 1100 hours March 17 the wind blew from the southeast at over 20 knots; at the same time the current flowed into the northwesterly quadrant at about 0.5 knot.

23

The Situation Reports disclose that the only severe pollution of beaches on the adjacent islands took place on the afternoon and evening of March 16 on Breton Island. Oil was carried onshore by the currents driven by the strong southeasterly winds.

Since the magnitude of tidal currents is approximately proportional to the tidal range, the diminishing current on March 19 probably reflects the oncoming equatorial tide of March 20.

The overall lack of correlation between the wind and the unreduced current observed at a depth of 5 feet suggests that the other current agents operating (tidal, relative, slope) are usually of the same magnitude or greater than the wind current contribution, effectively masking any relationships from all but a detailed analysis. It seems probable now that the 5-foot current does not reliably represent the surface current. It is unfortunate that the vertical ship motion and wave action prevented us from getting any detailed data closer to the surface than 5 feet.

Subsurface Currents.--Two further levels of the current observations during March 16-20 are shown in Figure 8. The general magnitude of the current speed differs little at the 25-foot level and the 45-foot level from that of the near-surface current. Speeds of 0.4 to 0.5 knot are most common at these depths. The current directions at the 25- and 45-foot levels, while remarkably similar to one another, differ sharply from the near-surface current directions in that they are reasonably steady. During most of this observation period these currents were moving toward the south-southwest. There is a possibility that these seaward-flowing currents were returning to the offshore water which was brought onshore by

the steady southeasterly wind. This seaward return flow effect at depth is quite clear on March 16 and 17, when the surface waters were moving onshore with the oil that washed onto Breton Island.

In summary, during the observation interval at the Dependable station, changes of current speed and direction below 10 feet are minimal. There is also a decided reduction in the tendency toward rotary flow in the lower layers.

Measurements (see appendix) from the C.G.C. Pt. Spencer in 40 feet of water on March 5 and 6 were made during the calmest period of the month; they clearly showed a clockwise rotating diurnal tidal current with minimum interference from wind currents. The current flowed initially south after high tide, turned westerly, and then flowed north about 13 hours after high tide. The average speed in the upper 10-foot layer was 1 knot; below this level the average speed was 0.5 knot. Directional turning of the lower layer lags slightly behind that of the upper layer.

Tidal Currents.--In order to isolate and examine the periodic tidal currents from the mixture of types comprising the observed current, harmonic analysis was carried out on the 5-foot level currents at the Dependable station March 16-19 and on the 5-, 15-, 25-, and 45-foot levels for March 18.

Harmonic analysis extracts the periodic components which can be accounted for by any set number of harmonics. The first two harmonics, namely the diurnal tidal current, with a period of 1 lunar day (24 hours, 50 minutes), and the semi-diurnal tidal current, with a period of 12 hours, 25 minutes, account for nearly 95 percent of the total periodic tidal current. As shown in Figure 10, we have used the first three harmonics in

25
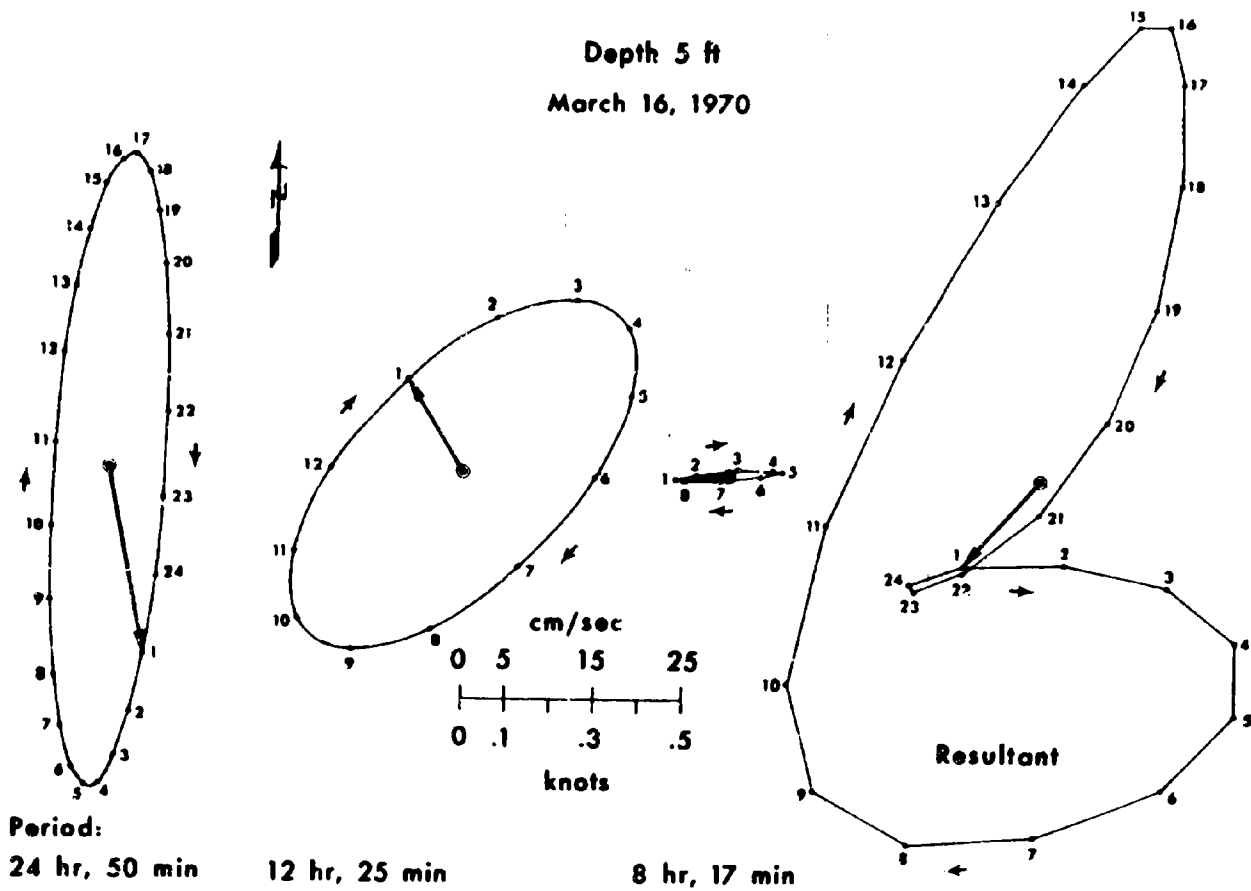
Figure 10. Tidal ellipses for first three harmonics and resultant tidal ellipse for 5-foot current.

our analysis. In this figure, which illustrates the method, the three diagrams to the left are the currents accounted for by the three harmonics individually--the irregular diagram on the right is the resultant current obtained by adding all the harmonics together. Such diagrams are called tidal ellipses; the current vector at any hour is given by an arrow drawn from the origin to the point labeled with that hour number. The length and direction of the arrow give the current speed and direction, respectively. On the graphs only the current vector at hour 1 is drawn. The smooth curve only serves as an envelope to connect the end points of the arrows. The semi-diurnal tide goes around its ellipse twice each day, etc. As the diurnal and semi-diurnal tide waves usually differ in magnitude, direction, and phase, the resultant tidal ellipse may be a rather compli- cated figure. As expected from our knowledge of the tides in the Gulf of Mexico, the diurnal tidal current is the most dominant. Because of the brevity of these records, it is not possible to assign an absolute time to the hourly notations on the tidal ellipses.

With the effects of steady currents removed, the tidal ellipses of Figure 11 show the day-to-day change in the tidal currents at the 5-foot level. The direction of rotation, as it should be in the northern hemi- sphere, is clockwise owing to Coriolis forces. There is an obvious decrease in the magnitude of the tidal current as time progresses because of the fact that we are nearly at equatorial tide on March 19 (the strength of the current is 1.0 knot on March 16 and only 0.6 knot on March 19). The orientation of the ellipse is generally in an onshore-offshore direction-- the maximum currents, then, are onshore and offshore with the flood and

27
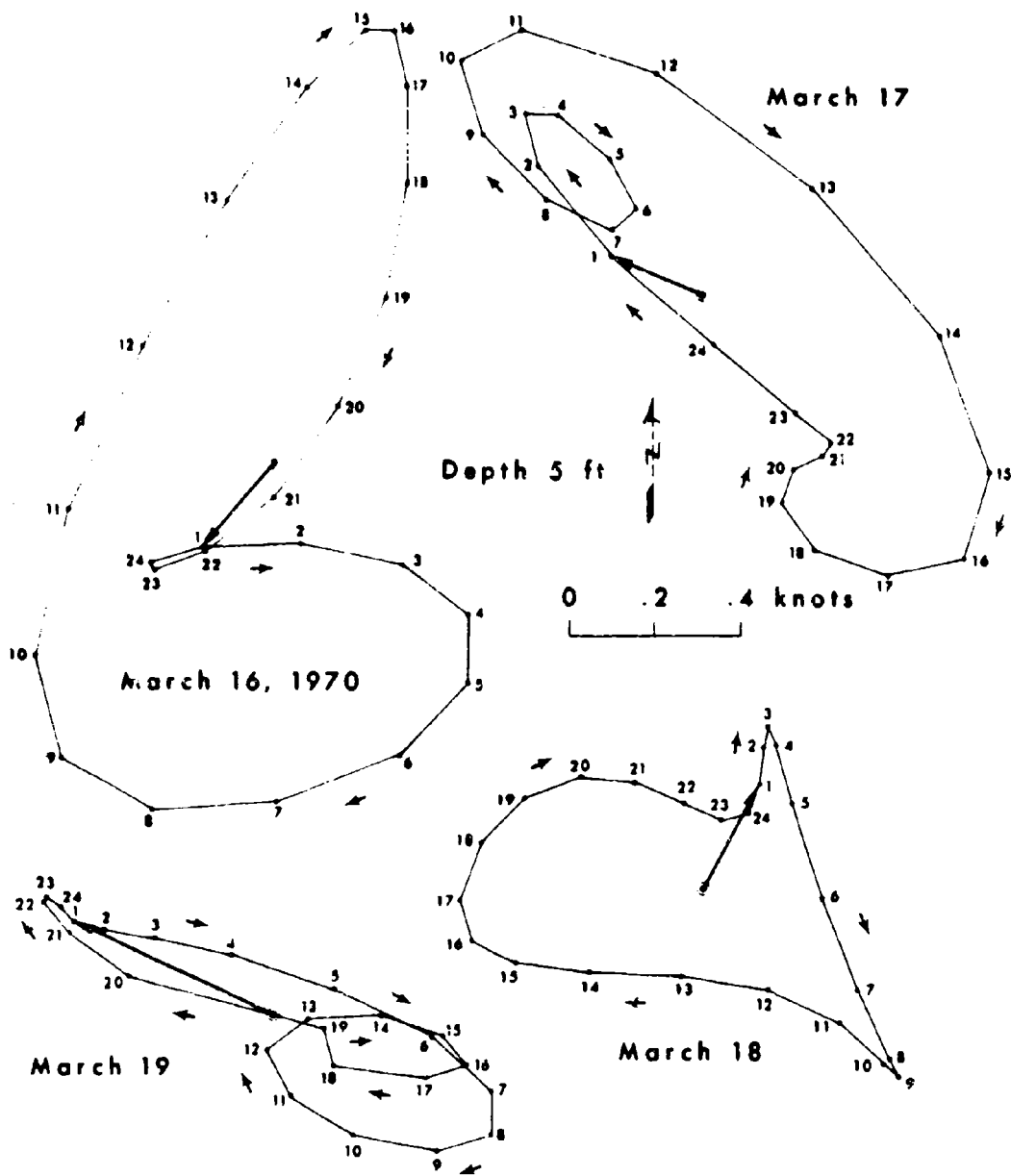
Figure 11. Resultant tidal ellipses for 4 days of current observations at Dependable station (5-foot depth).

ebb of the tide. This analysis has successfully removed a fairly typical tidal current from the rather confused data presented in Figure 6.

The changes in the tidal current ellipse as a function of depth are shown in Figure 12. Increasing frictional effects as the bottom is approached considerably distort the tidal current ellipse, resulting in occasional periods of counterclockwise rotation. Speeds are lower near the bottom and the higher speeds have a shorter duration.

It is apparent that oil purposely sunk into the bottom layers during equatorial tides would have the least aid from the tidal currents in dispersing.

Slicks

Figure 13, which is a plot of wind vectors against the slick vectors observed by helicopter visual surveillance, gives the distinct visual impression that there is a degree of correlation of wind direction and slick direction. A more detailed examination of the angle between simultaneous wind and current vectors is not possible owing to (1) uncertainties in the time of slick observations and (2) the fact that the only detailed wind data are restricted to the Dependable observations of March 15-20. It does seem clear from the figure, however, that after the wind has blown, say, a day from a given direction the slick aligns with the wind.

This relationship implies a good correlation between the movement of the upper foot of surface water and the wind. We have already shown that there is no clear relation between the current at the 5-foot level and the wind. Figure 14 shows the velocity profile predicted by Reid (1959) for a pure wind-drift current. There is a thin high-velocity

29
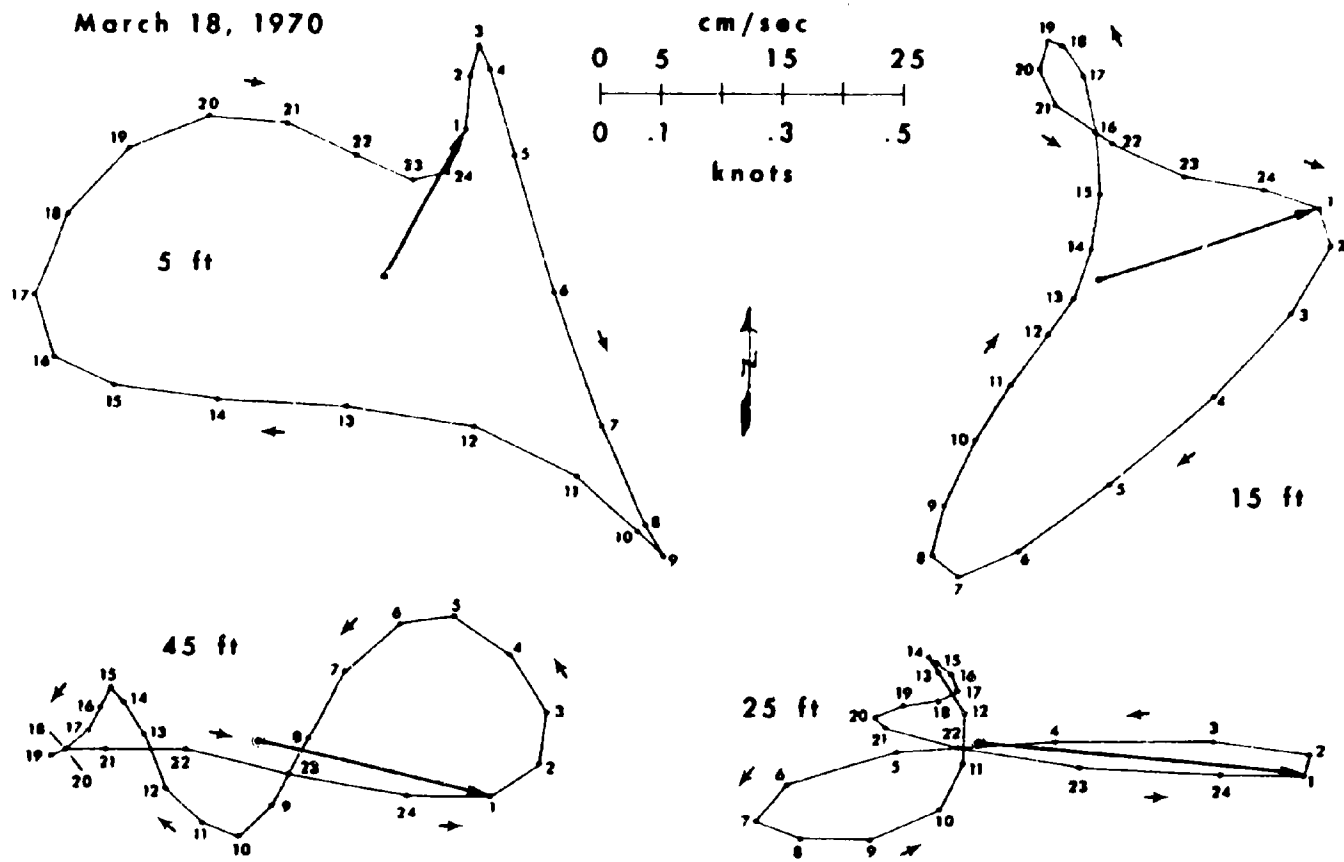
Figure 12. Resultant tidal ellipses at depths of 5, 15, 25, and 45 feet.
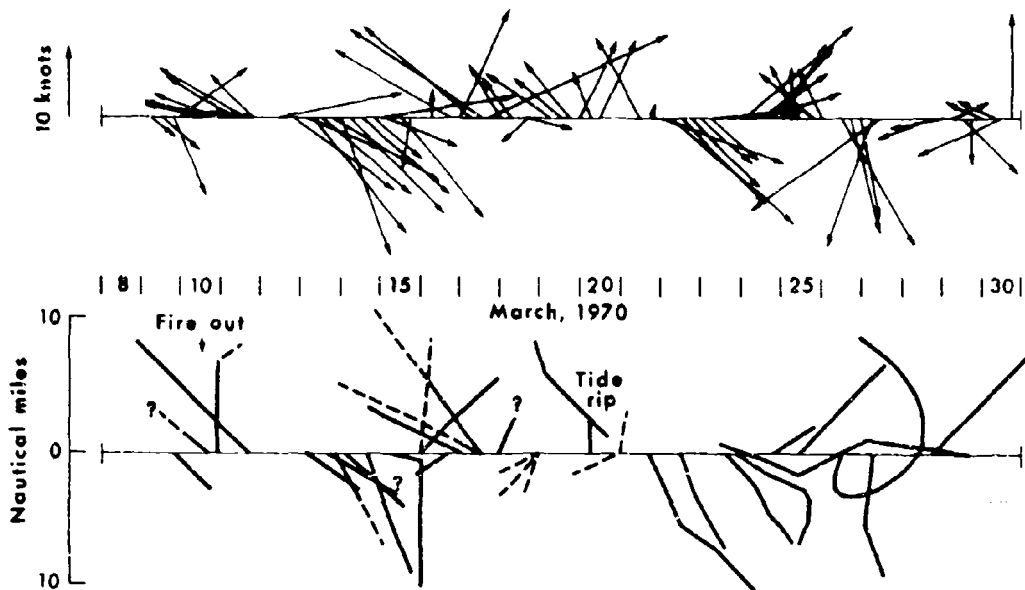
Figure 13. Wind vectors versus slick vectors.
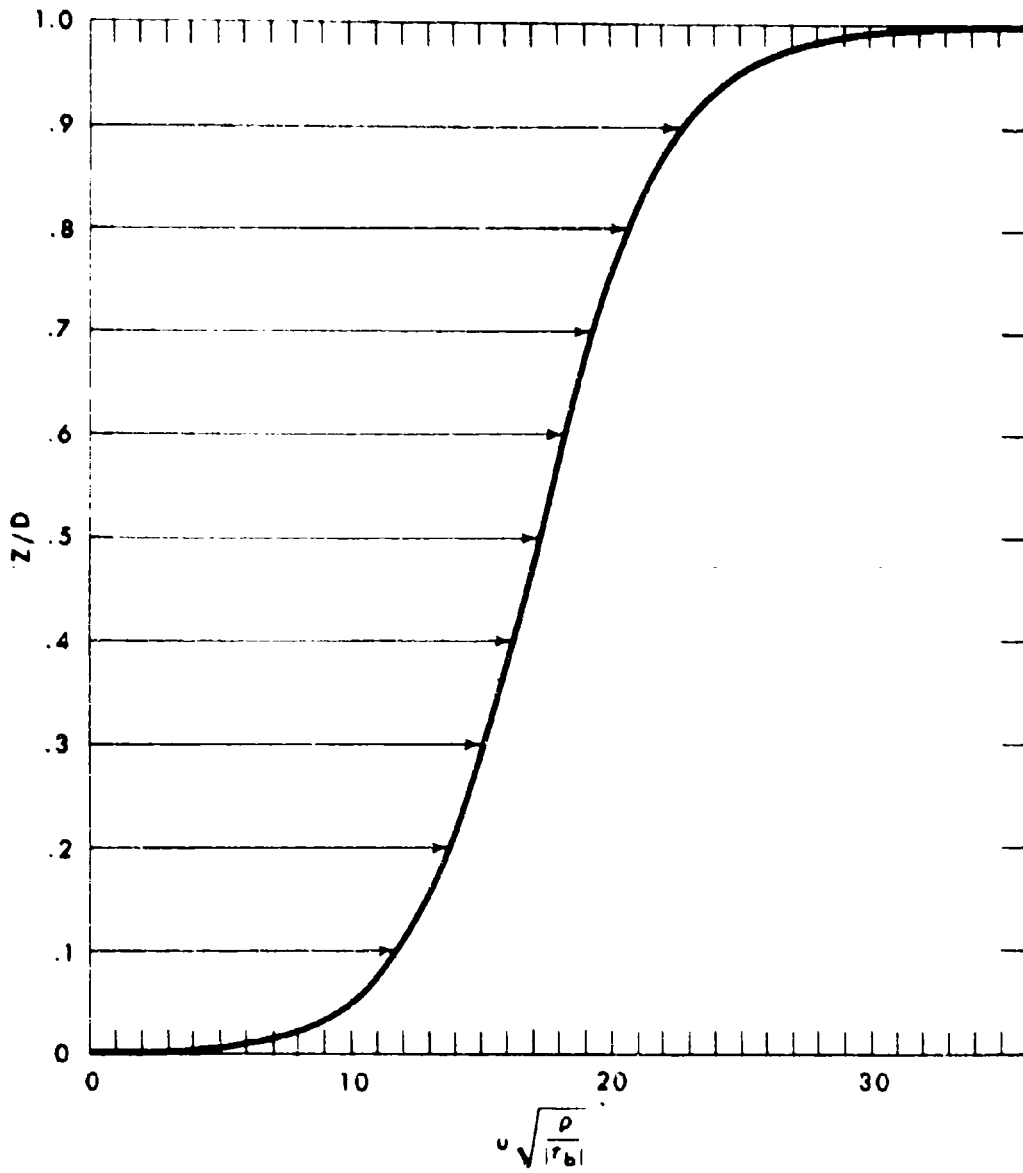
Figure 14. Non-dimensional vertical velocity profile for pure wind-drift current by Reid (1957). Z/D is relative depth, U is current speed, ρ is fluid density, and τ_b is shear stress uniform throughout the fluid.

layer predicted near the surface; it is this type of situation which would allow the very-near-surface water to move with the wind while the underlying waters (say, at 5-foot depth) are only barely affected. Some other means of monitoring currents closer to the surface is necessary to clarify the problem.

At times of high winds with steady direction, oil did definitely move with the wind, as was discussed in the section on currents with respect to the strong winds of March 16-17, which pushed oil onto Breton Island. The U.S. Geological Survey photomosaics and color photographs of oil slicks which were provided to us showed five cases in which oil slicks extended with the wind (within 20 degrees), as indicated by plumes of spray from the fire boats hosing down the platform (Fig. 15). Two cases showed no clear indication of wind direction, and one showed a slick extending at about 90 degrees to the wind direction.

As mentioned previously, slick orientation often changed abruptly at interfacial lines. Slicks also changed strikingly in shape at interfacial lines, becoming narrow bands (Fig. 16) of thicker oil accumulation, with coalescing "rafts" or "mats" of oil up to 1 centimeter thick. This change in shape of the slick and the observed stranding of other floating objects along the interface suggest that the boundary is a locus of downwelling at which floating materials collect. The slicks seem literally to contract to lie along the interface as if "swept" into a linear accumulation. The narrow accumulations are also sometimes distorted in patterns suggestive of very large Kelvin-Helmholtz waves, which may form along the interface of fluids in motion relative to each other.

33
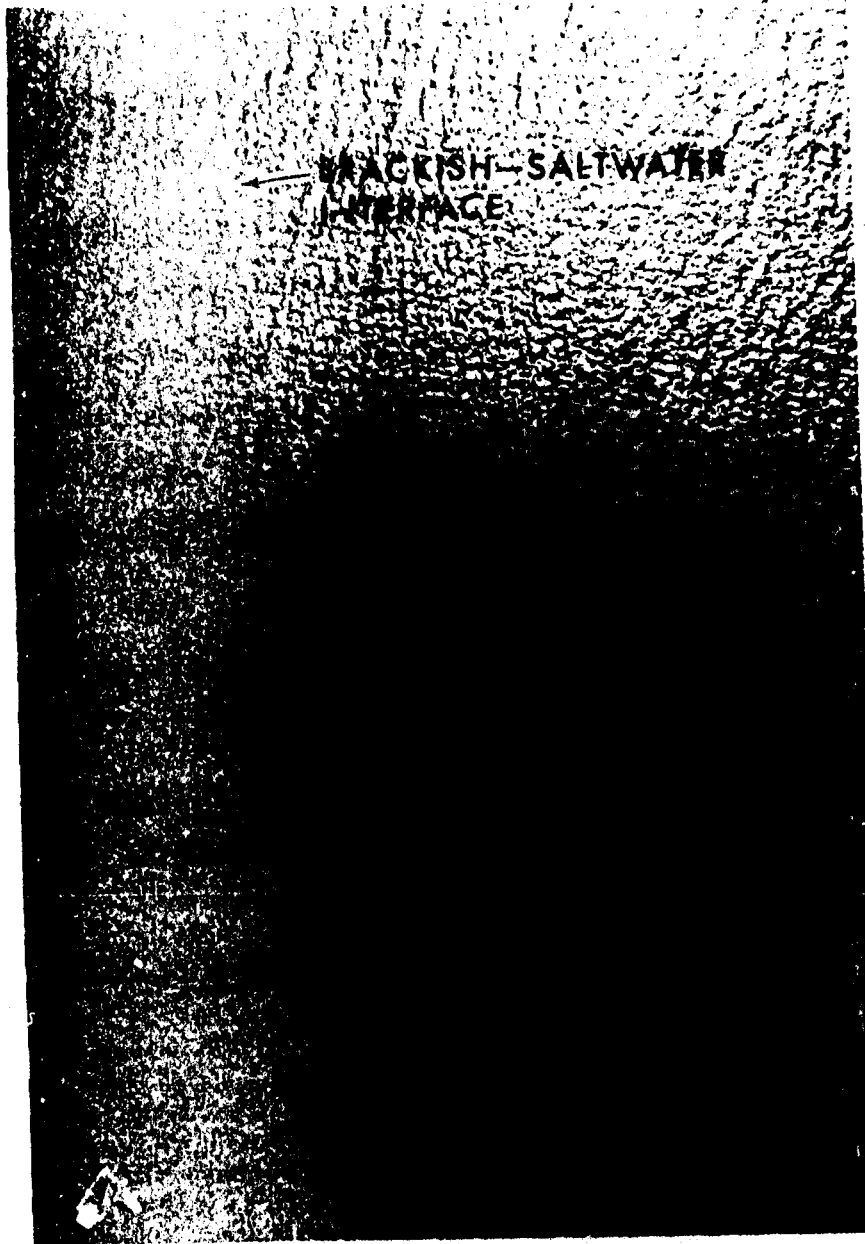
Figure 16. Narrow band of oil stranded along brackish water-saltwater interface. (Provided by U.S.G.S.)
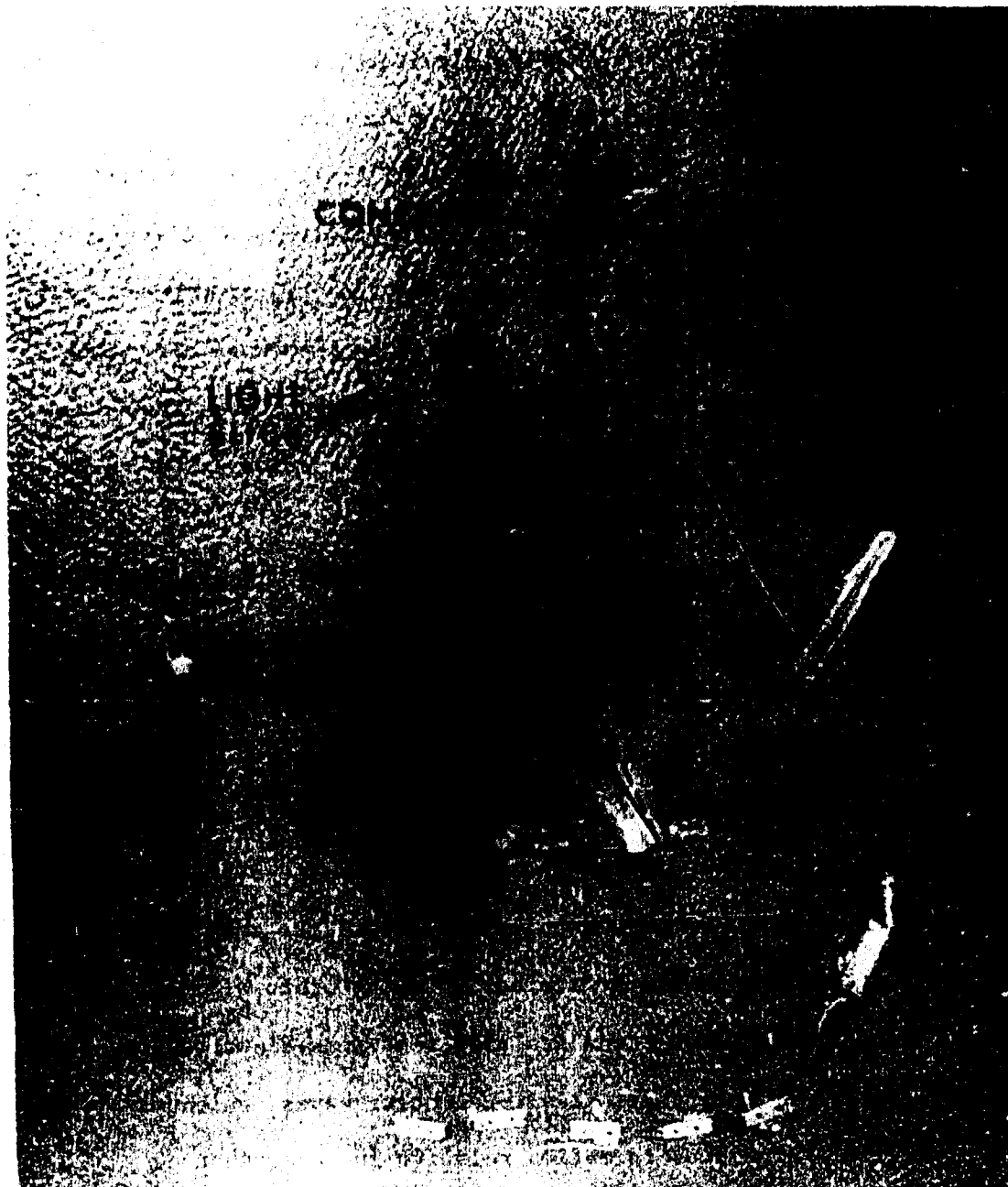
Figure 15. Photograph of slick, March 14, 1970. (Provided by U.S.G.S. Barge line was for trapping onshore-flowing oil. For direction and scale refer to Fig. 19.)

34

Where interfaces were not involved, slicks showed shapes that were straight or arcuate to varying degrees. The arcuate forms are indicative of currents, either tidal or wind generated, which rotated as the slick developed. Straight forms develop during periods of steady current direction.

The "mat" type of oil accumulation and the thin film slicks were the only types of floating oil noted. Some reports were heard at the time of thicker accumulations, but they were not substantiated by our observations.

The most useful images of oil slicks that were available for the study were those made by 8-14μ infrared scanning imagery. These showed the thin film as dark areas relative to the surrounding waters and the "rafts" of oil in thicker accumulations as bright areas. The same imagery showed excellent delineation of interfaces between different water masses as well. Sensitivity of this type of imagery at high altitude allowed sensing of the entire slick on a single image with adequate detail of size and shape. Future emergencies of this kind should be better documented by this type of sensing.

THEORETICAL CONSIDERATIONS--SLICK PREDICTION

Introduction

The mixing, dispersion, or diffusion of oil on the sea is undoubtedly a complicated process under field conditions because the process is largely controlled by changes in the weather and sea states. However, our understanding of the physical processes and ultimately of the spread of the oil can be greatly increased by application of the theory of turbulent diffusion. This approach has been successfully applied in the diffusion of atmospheric

36

polluntants and in studies of the spread of dye and other substances on lakes and on the sea.

Simple turbulent diffusion theory does not consider such effects as particle fallout, particle interaction, coagulation, or evaporation. Special terms may be added to the equations to account for these effects, however (see Yudine, 1959; McNown and Lin, 1952; and Sutton, 1953). Empirical determination of the diffusion coefficient K in the field during an oil spill should take these effects into account to some degree. The following development applies only to an oil slick dispersing in a laterally homogeneous water body. As shown in the previous section, horizontal density gradients and discontinuities will considerably distort the diffusion pattern.

Statistical Theory of Turbulence

In his pioneering paper of 1921 and again in a detailed treatise in 1935, G. I. Taylor developed the statistical theory of turbulence which laid the groundwork for most modern studies of diffusion problems in the atmosphere and ocean. By considering the one-dimensional spread of particles (or marked fluid parcels) from a continuous point source, Taylor developed the relation for the y direction

$$\sigma_y^2 = 2 \overline{v'^2} \int_o^T \int_o^t R_y(\xi) \, d\xi \, dt \tag{1}$$

where σ_y^2 is the variance of the fluid parcels around the source, $\overline{v'^2}$ is the square of the turbulence intensity, assumed to be constant over a period of several hours, $v' = v - \overline{v}$ as usual, ξ and t are time parameters, and

37

$R(\xi)$ is the Lagrangian autocorrelation function. For a detailed derivation of (1) see Haltiner and Martin (1959, p. 156). The Lagrangian autocorrelation function measures the relationship between the velocity of a parcel at one instant and the velocity of the same parcel at some subsequent instant.

$$R_y(\xi) = \frac{\overline{v'(t) \; v'(t-\xi)}}{\overline{v'^2}} \quad . \tag{2}$$

Hence for very short time lags $v'(t) \simeq v'(t-\xi)$ and $R_y(\xi) \simeq 1$. For long time lags there will be on the average no relation between $v'(t)$ and $v'(t-\xi)$; so $R_y(\xi) \simeq 0$. Similar expressions for $R_x(\xi)$ and $R_z(\xi)$ extend the Taylor analysis to three dimensions.

After considering very short times, performing the double integration, and then taking the first derivative with respect to time of σ_y, equation (1) reduces to

$$\frac{d\sigma_y}{dt} = (\overline{v'^2})^{1/2} \quad . \tag{3}$$

In the case of long diffusion times $\int_0^t R_y(\xi) \, d\xi = t_y^*$ a constant, and equation (1) reduces to

$$\frac{d\sigma_y^2}{dt}\bigg]_\infty = 2 \, \overline{v'^2} \, t_y^* . \tag{4}$$

The subscript ∞ refers to the ultimate constant value this quantity will attain. It a uniform horizontal mean flow is passing the source moving in the positive x direction at a speed U assumed constant over a period of several hours, the relation $T = x/U$ can be used to transform the spread of

38

the material into the x-y plane; so (3) becomes (for short diffusion times)

$$\frac{d\sigma_y}{dx} = \frac{(\overline{v'^2})^{1/2}}{U} \tag{5}$$

and (4) becomes (for long diffusion times)

$$\frac{d\sigma_y^2}{dx}\Big]_\infty = \frac{2\ \overline{v'^2}\ \ell_y^*}{U^2} \tag{6}$$

where ℓ_y^* the Lagrangian eddy size $= U\ t_y^*$. Thus $\frac{d\sigma}{dx}$ for short times and $\frac{d\sigma^2}{dx}$ for long times are both constants. Figure 17 illustrates the three ensuing diffusion regimes: (a) the linear or short-term regime, where $\sigma_y \propto x$, (b) the long-term regime, where $\sigma_y \propto x^{1/2}$, and (c) the intermediate or transitional regime, where $\sigma_y \propto x^n$, $1/2 < n < 1$. For the purposes of the illustration the area occupied by the dispersing material can be outlined by assuming that the radius to the visible edge of the slick (y = R) can be identified initially with some constant multiple of the root-mean-square displacement σ_y. It will also be assumed that the visible radius corresponds to an equal concentration C contour. Pritchard (1966) has expressed objection to this assumption in dye studies of diffusion processes, but because of the technical difficulty of obtaining cross slick measurements of the concentration C the assumption is at present unavoidable. An expanding slick should, then, initially exhibit a linear growth of its radius, followed ultimately by a slow parabolic expansion. We can logically apply the one-dimensional Taylor equations to an expanding oil slick because (a) oil is generally constrained by buoyancy forces to the surface (no

39
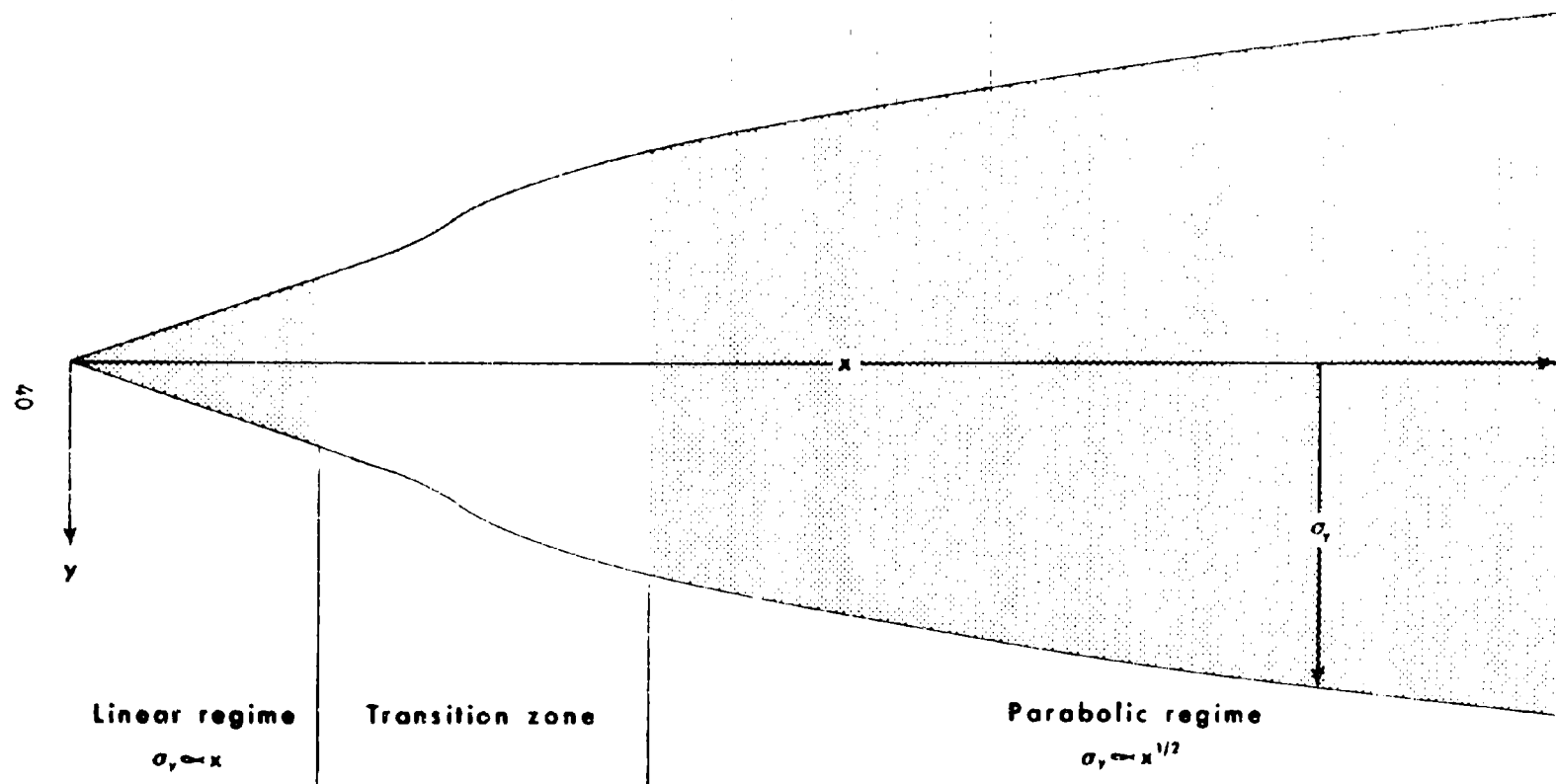
Figure 17.   Linear, transitional, and parabolic diffusion regimes predicted by Taylor theory.

mixing in the vertical direction) and (b) the longitudinal diffusion of the oil particles in the direction of the mean horizontal velocity is negligible compared to the displacements in this direction by the mean current itself.

Taylor has further demonstrated that the diffusion coefficient K_y can be expressed as

$$K_y = 1/2 \frac{d\sigma_y^2}{dt}\bigg]_{,,} = \frac{U}{2} \frac{d\sigma_y^2}{dx}\bigg],$$ (7)

or, substituting (6),

$$K_y = \frac{\overline{v'^2} \, \lambda_y^*}{U}.$$ (8)

Inspection of our own color and infrared color photographs, together with photographs and infrared imagery supplied to us by the U.S. Geological Survey and Remote Sensing Inc. of Houston, clearly and repeatedly shows the presence of the linear regime near the spilling well, 41C. This is exceptionally well shown in Figure 18. If we assume first that $\sigma_y = \alpha R$ (the root-mean-square displacement is directly proportional to the visible radius R) and as a first approximation that the proportionality constant α is near unity ($\sigma_y \approx R$), we can use the photographs and imagery to obtain estimates of the relative turbulence intensity of the oil from (5) and the diffusion coefficient of the oil from (7).

Table 1 lists the source and values for the relative turbulence intensity $(\overline{v'^2})^{1/2}/U$ of the oil, measured as the tangent of one-half the angle of expansion 2θ of the oil slick from the well.

Figure 18. Phot... ... ... stick illustrating initial linear expansion regime. (Provi... ... ...C.S. Long arm of barge line is about 1,920 feet.)

Table 1

Intensity of Turbulence Indicated by Oil

Source	$\tan \theta = \overline{(v'^2)}^{1/2}/U$
U.S.G.S. Infrared Color, undated	0.41
U.S.G.S. Color #0074, 3/14	0.25
U.S.G.S. Color #0003, 3/16	0.33
U.S.G.S. Color #0071, 3/14	0.28
U.S.G.S. B & W Mosaic, 3/22	0.22
U.S.G.S. B & W Mosaic, 3/13	0.22
Remote Sensing Inc., 3/14	0.22
Remote Sensing Inc., 3/11	0.10
Average	0.25

These results are encouraging, as it is well known (see, e.g., Kalinske and Pien, 1944; and Bowden, 1962) that the relative turbulence intensity in channel flow is in the range of 0.05 to 0.15. The effect of wave motions on the oil, especially breaking action, could certainly increase this value up to the observed average 0.25. Although the data points are few, a plot of $\tan \theta$ against wind speed in Figure 2 does seem to indicate a higher relative turbulence intensity of oil at higher wind speeds (stronger wave action).

Unfortunately, there is only one set of imagery which shows a slick with sufficient length and contrast to permit the measurements of the parabolic regime and so the determination of a value for the diffusion coefficient K_y. This is the Remote Sensing Inc. infrared imagery (8-14

scanner) of March 11, 1230 hours CST. The plot of σ_y^2 against x is shown in Figure 19. As predicted by (6), the linear relationship is strong; the regression coefficient = 0.97. With $d\sigma_y^2/dx]_\infty$ now known, use of (7) leads to an estimate of the diffusion coefficient of oil K of 4×10^5 cm^2/sec at that time. Since Figure 7 shows that wind speed and wave height were moderate on March 11, 4×10^5 cm^2/sec is probably a low rather than a high estimate. Comparison with the few published measurements of horizontal eddy viscosity (the diffusion coefficient for momentum) is encouraging. Sverdrup, Johnson, and Fleming (1942) report values (p. 485) ranging from 2×10^6 cm^2/sec in a small area with weak currents to 4×10^8 cm^2/sec in strong currents. It is now generally understood that the diffusion coefficient is a function of the scale of the phenomena under investigation. As Orlob (1959) clearly points out, the boundary of the field (basin), among other parameters, will restrict the maximum eddy size ℓ_y^* that may develop; and since K_y is related to ℓ_y^* by two other constants $K_y = (\overline{v'^2} \ell_y^*)/U$ (8), the diffusion coefficient in a bounded area should likewise approach a constant value.

It should be pointed out that the y coordinate of σ_y as one moves in the positive direction (downslick) does not necessarily follow an equal concentration contour. The evidence in Figure 19 does, however, seem to indicate that this is approximately the case for some distance downslick, until the concentration level at a distance σ_y from the average slick center line $C(y = \sigma_y)$ falls below the concentration level which is assumed to serve as a visible limit. In Figure 19 the discontinuity in the σ_y^2 versus x plot at $x \doteq 30,000$ feet is interpreted as that point where first

44
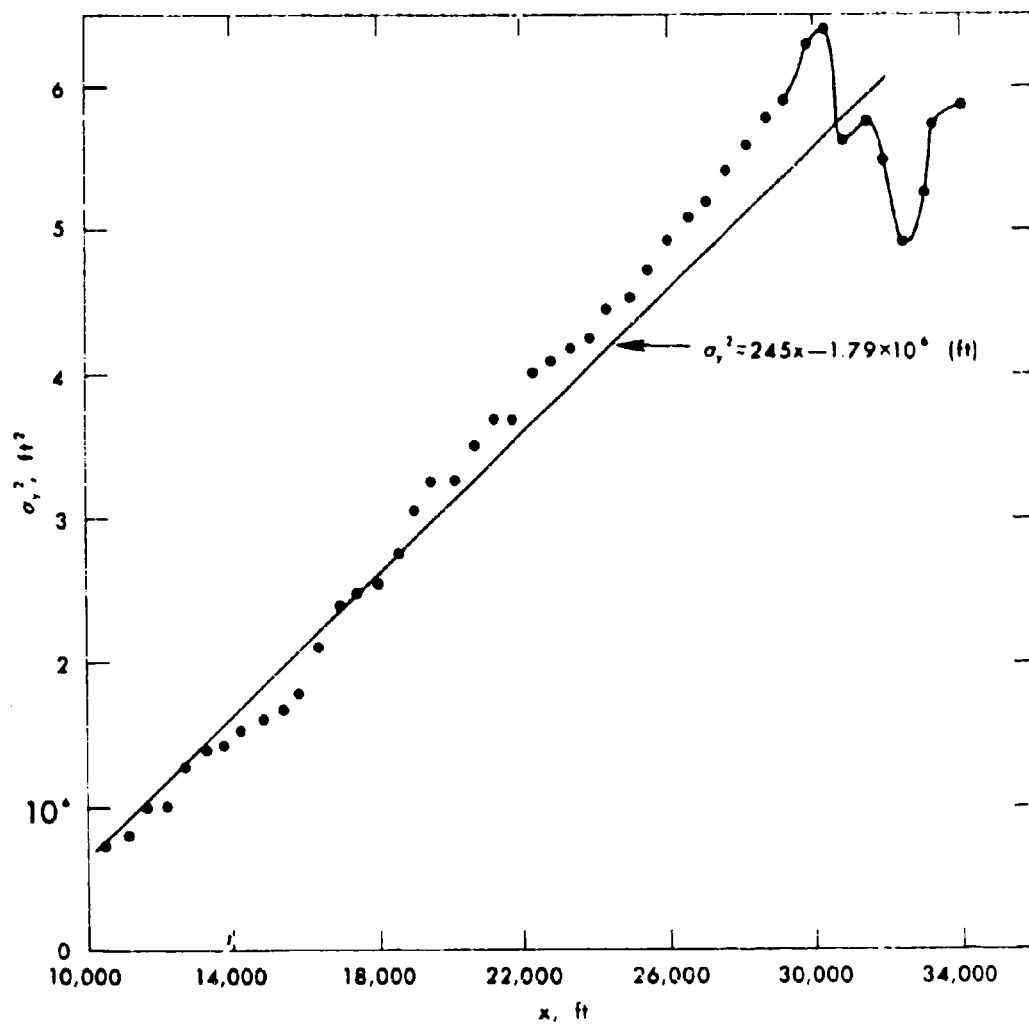
Figure 19. Plot of slick width variance (σ^2) against distance from source (x), illustrating linear relation that determines the diffusion coefficient.

$C(y = \sigma_y) < C(y = R)$.

Despite its power and apparent applicability to oil slicks, the Taylor theory cannot predict concentration contours or slick boundaries. For this we must turn to the classical diffusion equations.

General Diffusion Equations and Slick Prediction

Again regarding the spread of oil as a two-dimensional process in the x-y plane, with a near horizontal motion U in the postive x direction, the diffusion equation is

$$\frac{\partial C}{\partial t} + U \frac{\partial C}{\partial x} = \frac{\partial}{\partial x}\left(K_x \frac{\partial C}{\partial x}\right) + \frac{\partial}{\partial y}\left(K_y \frac{\partial C}{\partial y}\right) . \tag{9}$$

If the slick has come to steady state $\frac{\partial C}{\partial t} = 0$, and assuming (1) that the diffusion in bitropic $K_x = K_y = K$ and (2) that K has reached its constant value, (9) becomes

$$U \frac{\partial C}{\partial x} = K\left(\frac{\partial^2 C}{\partial x^2} + \frac{\partial^2 C}{\partial y^2}\right) . \tag{10}$$

For a derivation of the complete diffusion equation see Haltiner and Martin (1959, p. 265). The exact solution of (10) for a two-dimensional point source (infinite line source) in an infinite fluid is

$$C = \frac{Q \; e^{U \, x/2K}}{2\pi K} K_o\left(\frac{U \, r}{2K}\right) \tag{11}$$

where Q is the rate of emission of the source (g/sec), $K_o(\lambda)$ is, using standard notation, the modified Bessel function of 2nd Kind and Zero Order, and $r = (x^2 + y^2)^{1/2}$. For very reasonable values of U and K the first term

46

of the asymptotic expansion for $K_o(\cdot)$ (Abramowitz and Stegun, 1965, eq. 9.7.2; Roberts, 1923, p. 644) can be substituted in (11), yielding

$$C = \frac{Q\ e^{Ux/2K}}{2\pi K}\left(\frac{r}{Ur/K}\right)^{1/2}\ e^{-\frac{Ur}{2K}} . \tag{12}$$

Therefore

$$C = \frac{Q\ e^{-\frac{Ur}{2K}(1 - \cos\phi)}}{2\ (\pi K\ U\ r)^{1/2}} \tag{13}$$

where ϕ is measured in a clockwise direction from the positive x axis. Equation (13), then, is the expression we are seeking; it gives the distribution of the emitted oil as a function of distance and direction (r, ϕ) from the source, the rate of emission at the source Q, the ambient current speed U, and the oil diffusion coefficient K. The value of Q (personal communication, Commander Dixon, U.S.C.G.) during the Chevron incident is taken as 1000 bbl/day = 1241 g/sec.

Furthermore, following Roberts (1923) it can easily be shown that the maximum half-width of a given concentration contour is

$$y_{max} = \frac{Q}{(2\pi e)^{1/2}UC} \tag{14}$$

and by setting $\phi = 0$ in (13) the maximum extension downslick of a given concentration contour is

$$x_{max} = \frac{Q^2}{4\pi KUC^2} . \tag{15}$$

It is not difficult conceptually to relate the oil concentration C in g/cm^2 to the slick thickness. There may, in fact, be a direct relationship

47

if the hydrostatic equation $p = \rho gh$ is used. If C is identified with p (as they have the same dimensions), then the slick thickness h is directly proportional to C.

$$h = \frac{C}{\rho g} \,.$$ (16)

This idea, however, needs much closer examination.

One difficulty in using (13) to predict slick boundaries is that it predicts small but finite oil concentrations at infinitely great distances from the emitting source. In meteorology it is routine (Sutton, 1953) to take 10 percent of the maximum concentration as a visible boundary contour. Unfortunately, $C \to \infty$ at the origin in (13); so we must take some concentration close to the origin as a control level. Inspection of the solution of (13) along the center line of the slick ($\phi = 0$) for $K = 4 \times 10^5$ cm^2/sec, $Q = 1241$ g/sec, and $U = 50$ cm/sec (1 knot) shows that the presence of the source at $r = 0$ is just beginning to affect the solution adversely in the vicinity of $r = 100$ meters. The control concentration for the Remote Sensing Inc. (RSI) slick of March 11, with $K = 4 \times 10^5$ cm^2/sec, $Q = 1241$ g/sec, and $U = 50$ cm/sec, is, using (13), 0.7828×10^{-3} g/cm^2. The slick boundary $C_{y = R}$, then, is taken as 0.7828×10^{-4} g/cm^2. If this latter value for the concentration at the boundary is used, (14) predicts one-half the slick width and (15) predicts the slick length. The predicted maximum width of the RSI March 11 slick is 1,534 meters, the observed maximum width is 1,507 meters; the corresponding predicted length is 9,995 meters, while the observed length is 14,710 meters. The slick width is predicted more accurately than the length, but the results indicate the basic soundness of our approach. Furthermore, the average of 23 observations on slick

48

length made by Coast Guard helicopter visual surveillance teams, reported in the Situation Reports and displayed in Figure 13, comes out to 12,600 meters, compared to our prediction of 9,995 meters.

An exact expression for the area of a slick is not easily obtained from the basic equations; so we have resorted to an elliptical approximation

$$A = \pi ab \tag{17}$$

where a the semi-major axis is one-half the slick length given by (15) and b the semi-minor axis is the half width given by (14). Therefore

$$A \approx \frac{Q^3}{8 \sqrt{2\pi e} \; K \; U^2 \; C_{y = R}^3} . \tag{18}$$

Inspection of (14) shows that the slick width will increase directly with Q and decrease directly as U increases. It is noteworthy that (14) predicts that the slick width is independent of K. The slick length is more strongly dependent on Q, increasing as Q^2 and decreasing directly as U or K increases. The area given by (18) increases as Q^3 and decreases as U^2 and the first power of K.

The effect of varying U, with Q and K held constant, is shown in Figure 20. Low values of U produce a long, large slick; values of U approximately equal to those observed in the field during the Chevron incident (0.6-0.8 knot) produce relatively short and slender slicks much like those repeatedly observed in photographs and visually. The estimated time t required to reach a steady state is also shown in Figure 20. This is crudely approximated as the time required for oil to travel with the current out to

49

Area=12.2 km²

t=5.5 hours

U=1 knot

Louisiana slick

March 11, 1970

U=.6 knot

Area=48.2 km²

t=22.2 hours

U=.5 knot

Area=301 km²

t=5.7 days

U=.2 knot

0   10   20 km

Theoretical slicks: K=4×10⁵ cm²/sec

Q=1000 bbl/day
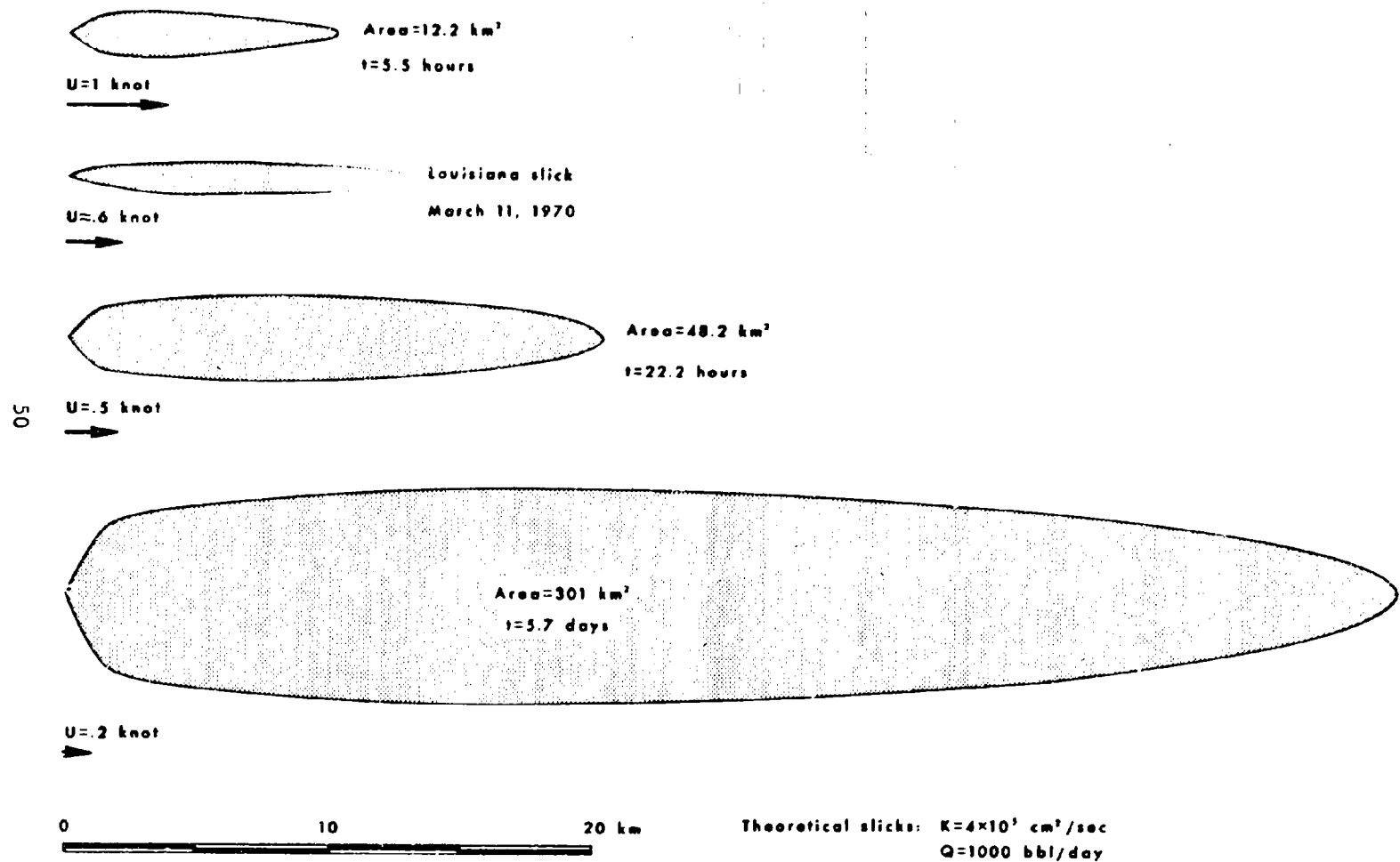
Figure 20.   Comparison of observed slick against theoretical slicks, illustrating effect of decreasing current velocity on slick size.

the outermost slick boundary. A numerical solution of the time dependent differential equation should produce a considerably more accurate estimate.

The shape factor SF of the slick, defined as the ratio of slick width to slick length, is, combining (14) and (15),

$$SF = \frac{4\ (2\pi)^{1/2}\ K\ C_{y\ =\ R}}{Q\ e^{1/2}}\ .$$

It is noteworthy that the relative shape of the slick is independent of the current speed, being controlled solely by (K/Q) for a given boundary concentration. Low values of (K/Q) produce elongate slicks; high values of (K/Q) produce more circular slicks. For the Chevron incident, using $K = 4 \times 10^5$ cm^2/sec, $C_{y\ =\ R} = .78 \times 10^{-4}$ g/cm^2, and $Q = 1241$ g/sec, the predicted value of the shape factor SF = 0.15. Table 2 lists the shape factors determined from slick geometries reconstructed from U.S. Coast Guard helicopter visual surveillance Situation Reports. Unfortunately, only data from the last week of the incident were of sufficient detail to be of use in this regard.

Table 2

Shape Factors During Chevron Incident

Date	Time	Shape Factor
3/26	0011 Z	0.50
3/26	1756 Z	0.19
3/29	0140 Z	0.22
3/29	1905 Z	0.07
3/30	1521 Z	0.17
3/30	1940 Z	0.16
3/31	2030 Z	0.32
Average		0.23

51

The approximate agreement of the average SF with the predicted value of 0.15 suggests that the value of K on the average should be closer to 6×10^5 than to 4×10^5 cm^2/sec for the last week of March.

Figures 21 through 27 present in more detail and in graphic form most of the results we have discussed up to now. Figures 21, 22, 23, and 24 show slick area as a function of Q, K, and U, whereas Figures 25, 26, and 27 show slick width and slick length as functions of these same three variables. In further studies along these lines an effort should be made to incorporate these parameters into a single nondimensional diagram or nomogram.

Although this two-dimensional diffusion approach seems to present a good approximation of gross slick geometries, it is really based on the concentration value at the slick boundary, for which we made only a rough estimate (10 percent of C at $r = 100$ m, $\phi = 0$). In future work this point must be examined in much greater detail.

SUMMARY

Observations prior to and during the long period of continuous oil spillage from a Chevron production platform near the Mississippi Delta permit certain generalizations to be made about movement of oil in coastal shallow water bodies. An understanding of the situation seemed to require information on currents, winds, tides, waves, and orientations and shapes of spreading oil masses. Salinity and temperature structure of the surrounding waters seemed useful for indicating the riverine and marine influences expected in the delta. Information was gathered on all of these in the hope that understanding could be gained of the principal agents which control rates and direction of motion of oil on water.

52
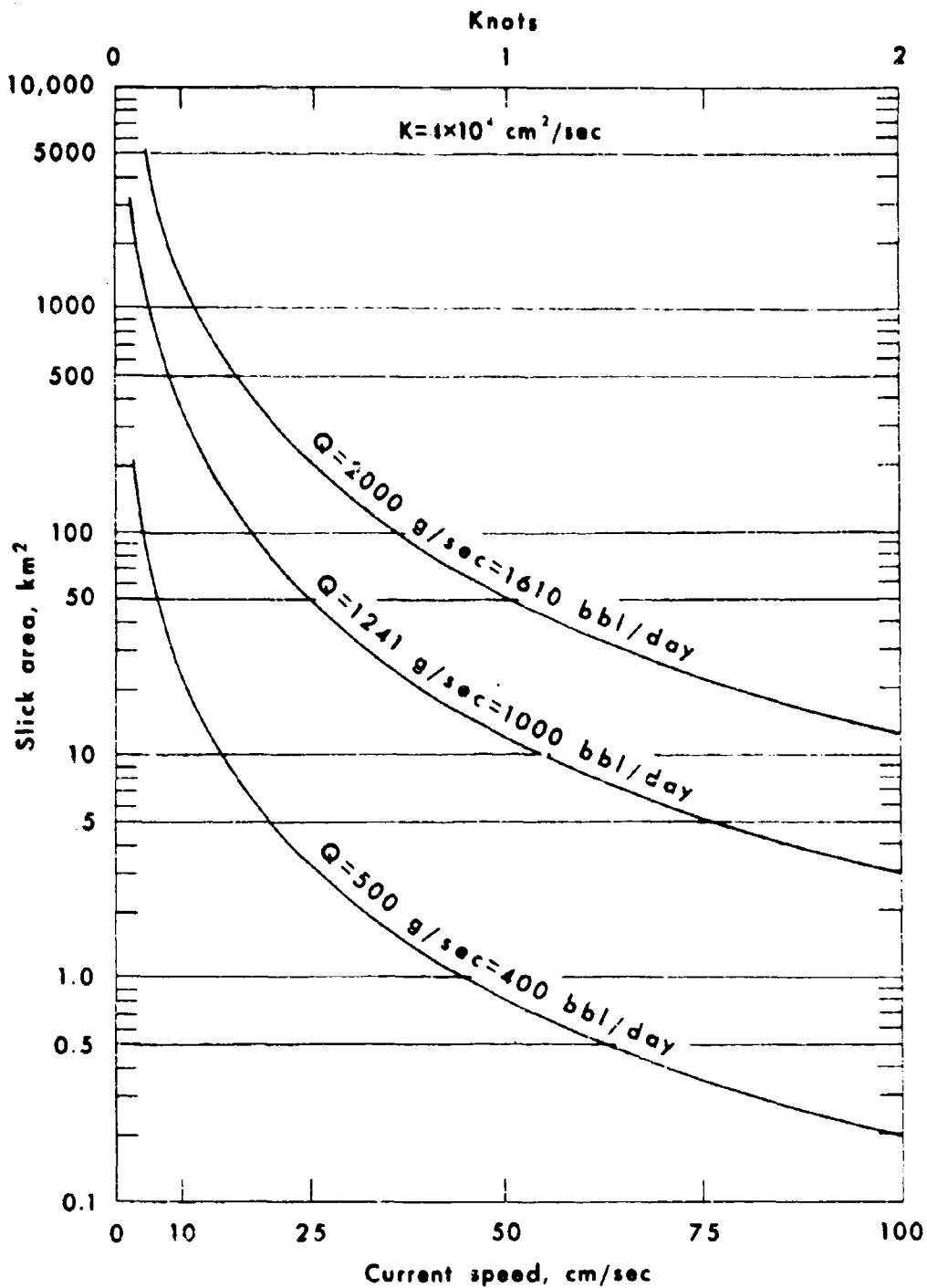
Figure 21. Slick area (A) as a function of current speed (U) for various rates of oil discharge (Q).
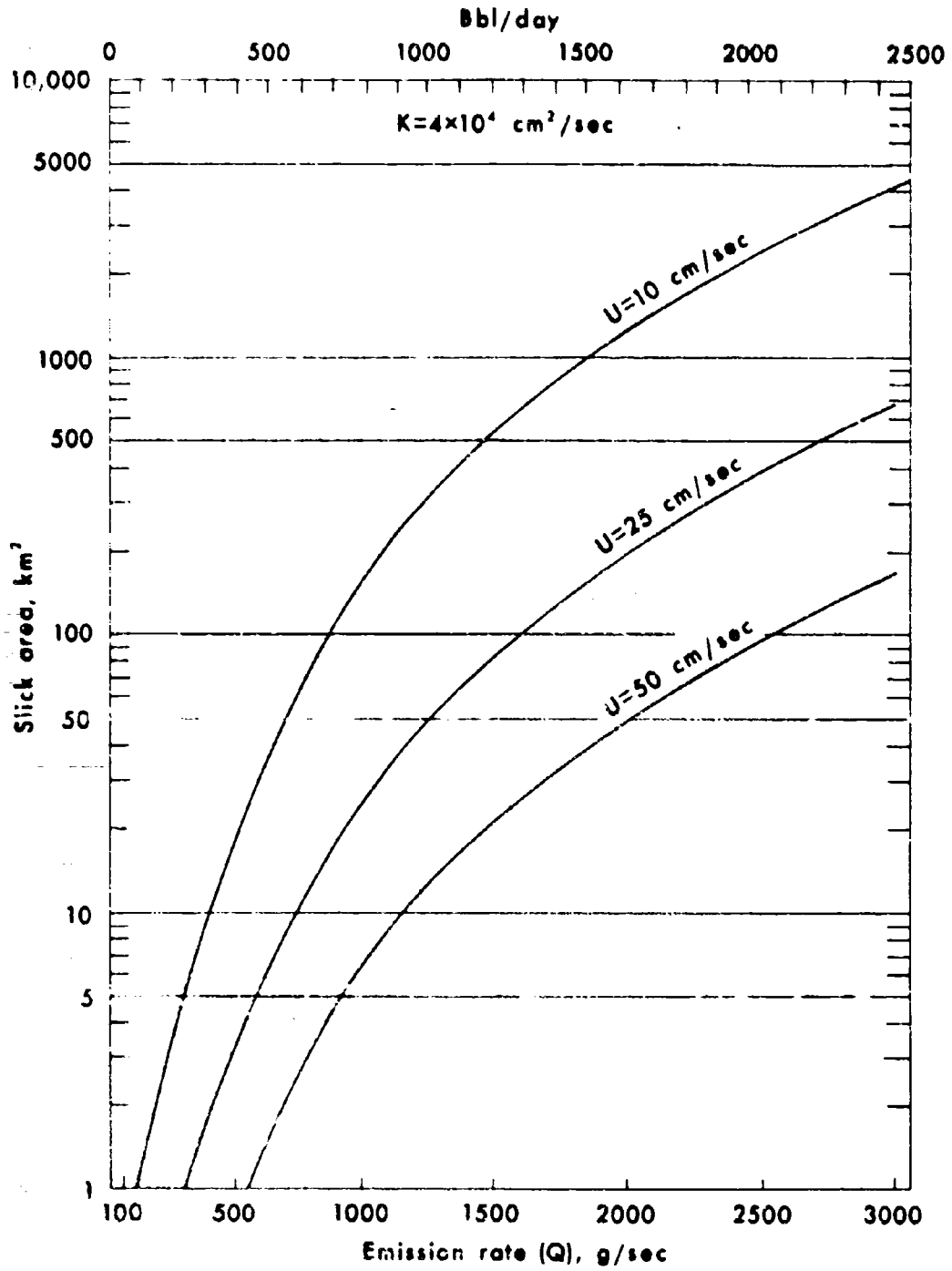
Figure 22. Slick area (A) as a function of oil discharge (Q) for various values of current speed (U).

54
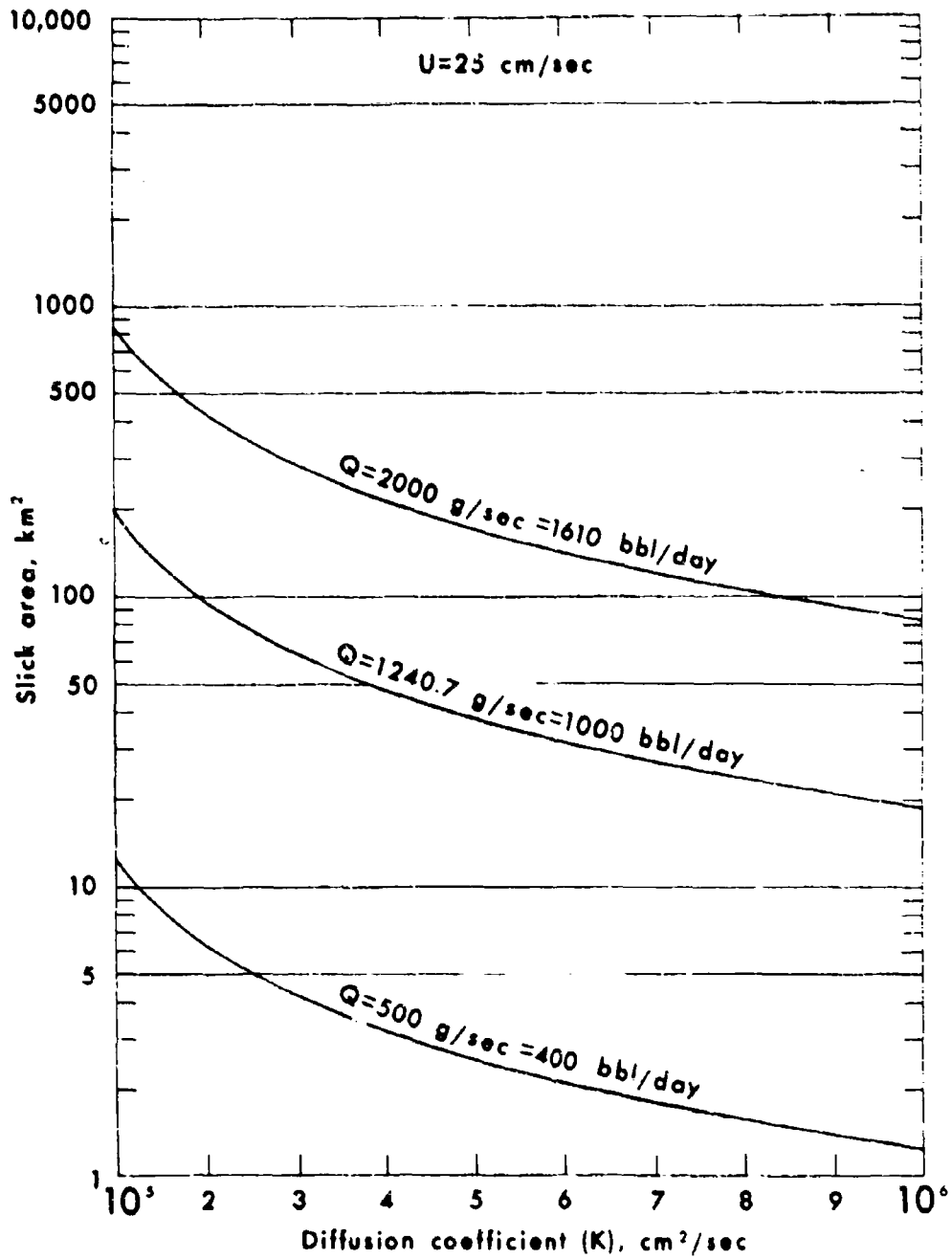
Figure 23. Slick area (A) as a function of diffusion coefficient (K)
for various values of discharge (Q).

55
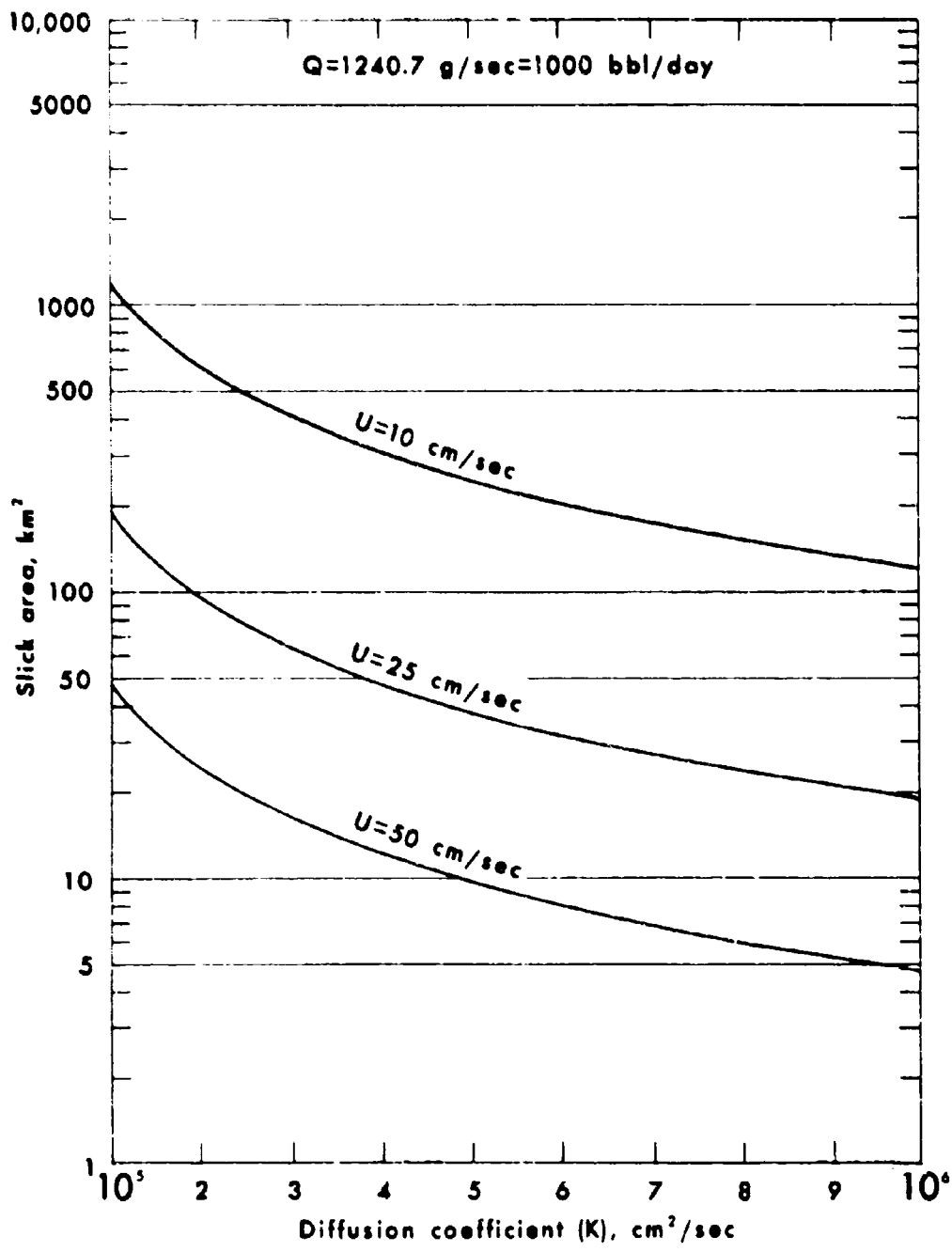
Figure 24. Slick area (A) as a function of diffusion coefficient (K) for various values of current speed (U).

56
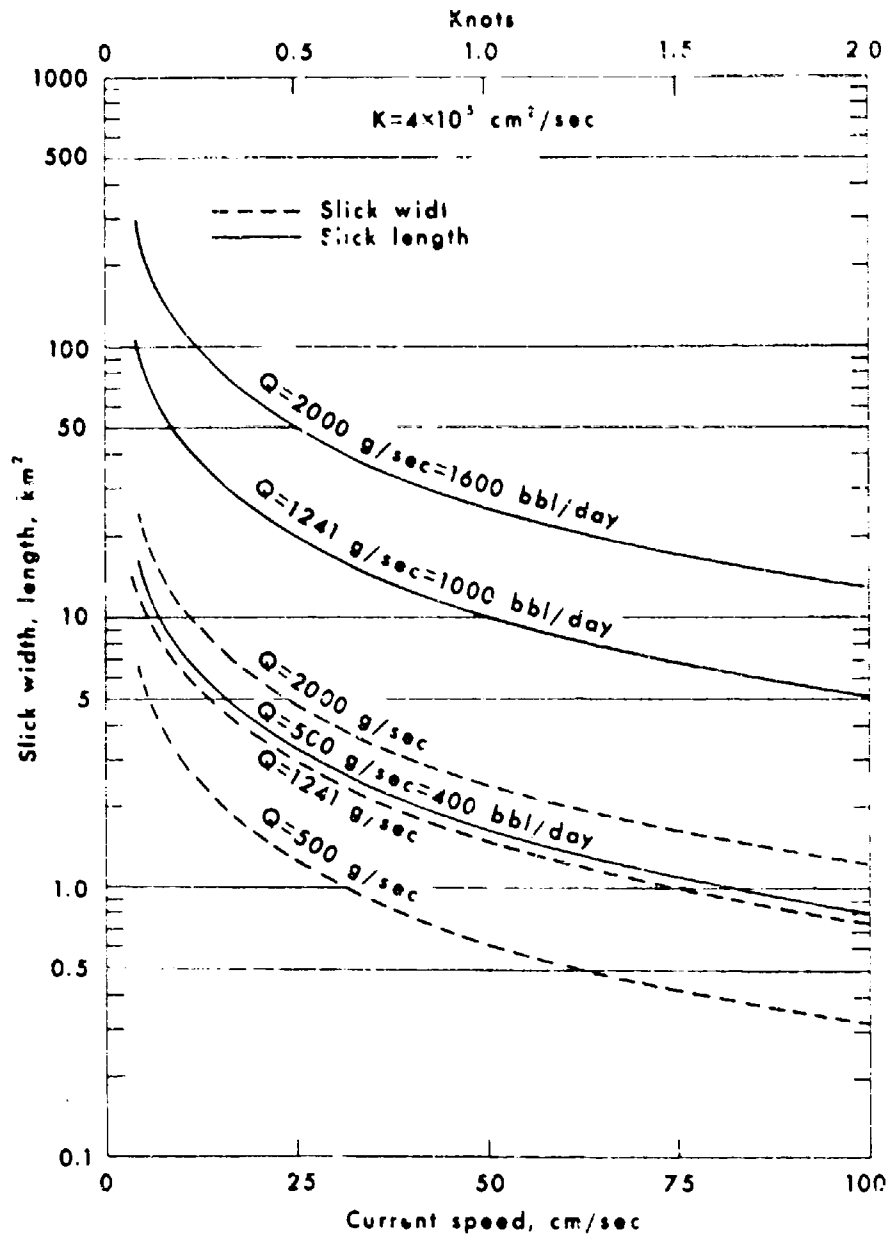
Figure 25. Slick width (W) and slick length (L) as a function of current speed (U) for various values of discharge rate (Q).
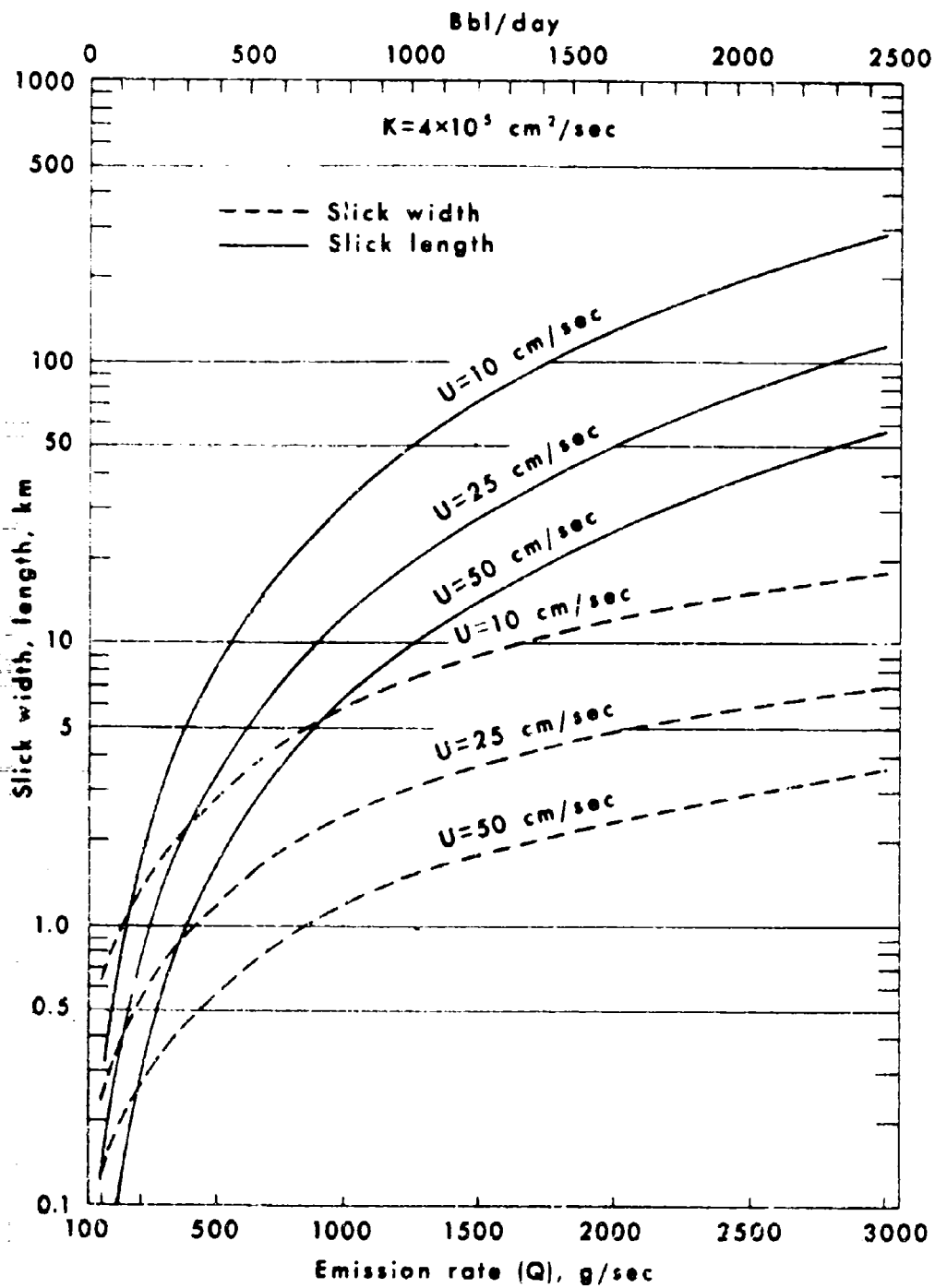
Figure 26. Slick width (W) and slick length (L) as a function of rate of discharge (Q) for various values of current speed (U).

58
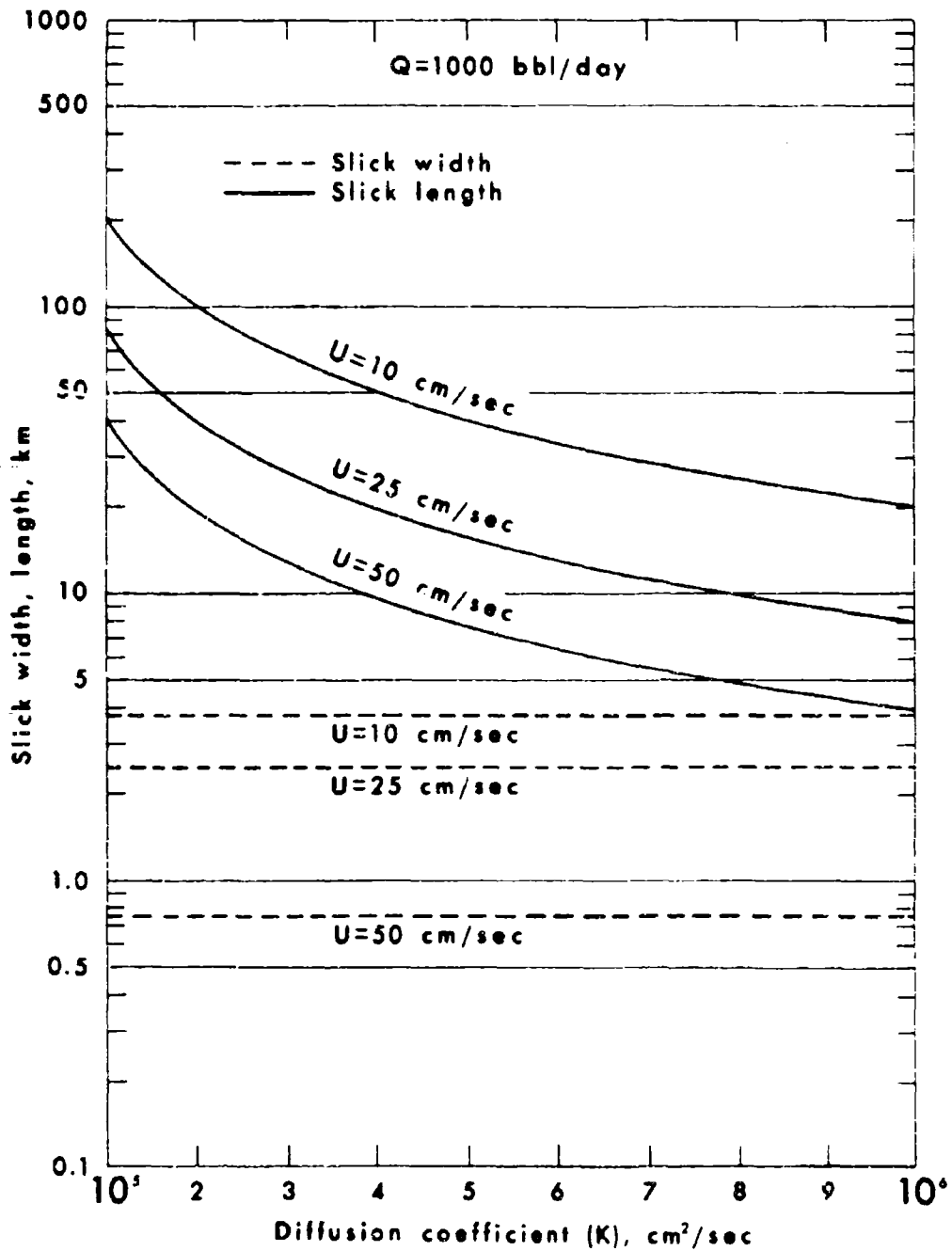
Figure 27. Slick width (W) and slick length (L) as a function of diffusion coefficient (K) for various values of current speed (U).

59

Winds during March were somewhat more varied than would be expected from long-term records. Strong winds to the southeast, which are usually rather infrequent in March, were probably important in reducing the amount of oil reaching shore.

At least once each week winds were sufficiently strong to generate waves of 2 to 4 feet, significant wave height. Two such periods of wave buildup and decay were documented by our instrumentation. There is no doubt that the stirring and mixing caused by these waves played a significant role in the continued breakup and diffusion of the oil slicks.

Salinity and temperature in the upper 15 feet of the water column showed rapid and strong variation. These were related to masses of turbid lower salinity water deriving from the river mouths. Interfaces between the river-derived and marine water masses were usually sharp and acted as barriers to movement of oil by other agents. The large amount of water being discharged from the Mississippi during March was one of the more important deterrents to movement of oil into the marshes because of this barrier effect, plus the escape of discharged river water out to sea.

Observations on the local tides indicated that they agreed very well with those predicted at Pensacola. The current observations, on the other hand, showed a complicated pattern; although tidal components were strong, their interaction with wind-drift currents and slope currents masked any clear relationship between the tide and the current or the wind and the current. Harmonic analysis of the currents did isolate typical current ellipses which had strong diurnal and semi-diurnal components (0.5-1.0 knot). This analysis further showed that the amplitude of the tidal current decreased

60

with decreasing tidal range (as the time of equatorial tides approached) and increased with distance from the bottom.

A general association of slick movement with wind direction is indicated from aerial photographs and from Coast Guard Situation Reports. Oil washed ashore on Breton Island on March 16 and 17 in a period of strong winds blowing from the well to the island. This was the main period when oil reached shore. The indicated association of slick movement with wind is in contrast with the lack of correlation between the wind and the current at the 5-foot level. One possible explanation suggested by theory is that the slick was embedded in a thin, high-velocity surface driven by the wind stress.

Slick shapes and orientations were often controlled by long (up to several miles) lines or zones separating brackish water masses from those of normal Gulf salinity. There apparently was no horizontal component of motion across these interfaces, as oil and other material frequently accumulated along them. These discontinuities often formed a natural barrier, preventing oil from moving onto the shore.

A theoretical analysis was undertaken to ascertain the effects of the rate of oil discharge, the ambient current speed, and the rate of oil diffusion on the area, width, and length of an ideal slick. Typical values for the Chevron incident predict an equilibrium or steady-state slick length of about 10 kilometers in length and 1.5 kilometers in width. These values agree very well with the on-site observations. Other results on the theoretical analysis are as follows: (1) For a given oil spill

incident the current speed largely determines the size a slick will reach; (2) the ratio of the diffusion coefficient to the rate of oil discharge controls the shape of the slick; (3) high discharges will provide elongate slicks; and (4) the consistently high current speeds during the Chevron incident kept the slick size to a minimum and greatly enhanced the rate of diffusion of the oil.

CONCLUSIONS

1. In the waters surrounding the Chevron MP-41C platform it is apparent that wind stress tends to drive a thin layer of surface water before the wind. This is indicated by the frequent agreement of slick orientation with wind direction.

2. Detailed measurements of currents at 5-foot depth did not show agreement with slick orientations or wind directions except for periods of higher wind speeds.

3. Harmonic analysis removed significant diurnal and semi-diurnal components from the current records. The remaining non-periodic components largely lect a combination of wind-generated currents and slope currents from setup, setdown, and river discharge.

4. Tidal currents showed a strong dependence on the range of tide, with the speed dropping by a factor of 2 or 3 from tropic tide periods to equatorial tide periods. Dispersion of oil could be expected to diminish accordingly.

5. Currents at depth showed a greater importance of non-periodic components; and, although rotational effec , were still evident, the deeper currents frequently ran counter to the near-surface currents. The trajectory of chemically dispersed oil could therefore not be predicted from

62

surface observations.

6. The sharp boundaries associated with lower salinity water masses moving through the area were sites of oil stranding and accumulation.

7. Theoretical analysis indicates a strong effect of current speed on slick size. The high speeds of the Chevron incident rapidly diffused the oil and kept slick sizes to a minimum. Slick size and shape also varied as a function of rate of oil discharged and the coefficient of diffusion, which was empirically determined to be 4×10^5 cm^2/sec for the Chevron case.

ACKNOWLEDGMENTS

APPENDIX

Station	Date	Profile	Depth	Salinity	Temperature	Current Speed	Direction	Time
Pt. Spencer	3/5	1	2.5	31.5	16.2	1.0	162	2245
Station 1			5	31.1	16.3	.70	154	2235
			10	32.7	16.3	.50	162	2220
			15	34.0	16.5	.15	234	2215
			20	34.7	16.3	.10	360	2200
			25	34.9	15.9	.10	360	2150
			35	35.7	15.5	.20	360	2125
		2	2.5	27.4	16.45	1.2	180	2355
			5	30.7	16.6	.75	180	2348
			10	32.3	16.4	.55	216	2342
			15	34.5	16.3	.40	216	2334
			20	34.4	16.5	.25	198	2325
			25	35.2	15.9	.15	234	2315
			30	35.0	15.7	.20	225	2305
			33	35.4	15.8	.15	306	2255
	3/6	3	2.5	22.49	15.88	1.4	171	0103
			5	27.15	16.18	.75	180	0056
			10	32.50	16.18	.55	144	0044
			15	34.08	16.76	.45	216	0035
			20	34.42	16.30	.30	198	0028
			25	35.51	15.68	.20	198	0018
			30	35.65	15.88	.18	180	0015
			36	35.51	15.65			0007
		4	2.5	18.30	15.85	.75	216	0225
			5	20.0	16.00	.75	221	0215
			10	32.29	16.05	.75	180	0203
			15	34.19	16.25	.50	216	0153
			20	34.34	16.58	.38	234	0147
			25	35.20	15.82	.25	216	0141
			30	35.50	15.60	.30	198	0127
			35	35.64	15.62	.23	162	0124

Station	Date	Profile	Depth	Salinity	Temperature	Current Speed	Direction	Time
		5	2.5	21.46	16.15	1.5	261	0345
			5	21.41	16.01	1.0	252	0335
			10	32.03	15.82	.65	252	0325
			15	32.43	15.83	.45	216	0312
			20	34.15	16.48	.35	198	0304
			25	35.03	16.15	.30	180	0253
			30	35.32	15.62	.30	162	0247
			35	35.75	15.50	.20	108	0240
		6	2.5	29.12	16.13	.75	288	0510
			5	28.75	16.00	.75	252	0500
			10	28.71	15.98	.65	198	0445
			15	31.48	15.90	.45	180	0435
			20	33.58	16.02	.35	144	0425
			25	34.86	15.86	.2	180	0420
			30	35.27	15.48	.15	144	0410
			35	35.50	15.68	.05	108	0355
		7	2.5	30.97	15.90	.75	360	0620
			5	30.95	15.88	.75	360	0610
			10	30.84	16.05	.60	270	0600
			15	32.63	15.67	.10	198	0550
			20	33.57	15.74	.05	144	0535
			25	34.91	15.70	.05	117	0525
			30	35.25	15.82	.05	90	0520
		8	2.5	31.22	16.17	1.0	360	0725
			5	31.22	16.01	.95	360	0718
			10	31.12	16.05	.85	328	0713
			15	31.22	16.08	.65	288	0705
			20	31.88	16.0	.20	216	0655
			25	34.55	15.88	.15	108	0646
			30	35.01	15.55	.15	72	0635

99

Station	Date	Profile	Depth	Salinity	Temperature	Current Speed	Direction	Time
		9	10	31.62	16.10	.75	360	0812
			15	31.82	16.09	.60	328	
			20	33.0	15.79	.20	25	0757
			25	34.2	15.6	.20	198	0745
			30	35.08	15.5	.15	144	0740
		10	5	32.85	16.24	.70	288	0955
			10	33.21	16.25	.60	288	0947
			15	32.97	16.11	.45	252	0938
			20	33.52	15.74	.15	252	0932
			25	34.05	15.40	.25	198	0925
			30	34.4	15.59	.20	180	0915
		11	5	33.24	16.26	.75	288	1041
			10	33.25	16.22	.75	270	1035
			15	33.24	16.28	.55	198	1027
			20	33.20	16.11	.25	180	1018
			25	34.07	15.58	.05	180	1010
			30	35.18	15.47	.05	252	1004
Pt. Spencer Station 2	3/10	1	2	8.18	13.70			0640
			5	26.58	15.04	1.0	18	0634
			10	33.45	14.92	1.25	40	0640
			15	34.57	15.04	.80	18	0645
			17.5	35.36	15.40			0655
			20	36.01	15.76	.50	18	0708
			25	35.96	15.96	.50	360	0715
			27.5	35.98	15.82	.45	360	0720
			28.5	35.93	15.85	.40	360	0725
			30	35.99	15.83	.35	360	0728
		2	2.5	7.23	14.06	.75	360	0835
			3.0	16.77	15.26			0843

67

Station	Date	Profile	Depth	Salinity	Temperature	Current Speed	Direction	Time
			5.0	33.27	15.57	1.25	30	0830
			10	34.42	14.78	1.0	36	0820
			15	35.45	15.56	.85	36	0813
			20	35.92	15.82	.6	360	0807
			25	36.03	15.87	.5	360	0800
		3	2.5	16.55	14.93	.75	360	0935
			5	33.17	15.45	1.0	36	0934
			10	34.27	15.38	.80	36	0920
			15	35.40	15.60	.75	18	0903
			20	35.83	15.82	.60	360	0847
			25	35.99	15.85	.55	360	0853
			30	36.18	15.83	.35	360	0847
		4	2.5	10.60	15.33	1.0	360	1030
			5	31.27	15.36	1.1	15	1040
			10	35.35	15.34	.8	15	1045
			15	35.68	15.82	.65	18	1050
			20	36.09	16.14	.55	360	1105
			25	36.15	16.10	.60	360	1117
			30	35.92	15.91	.40	360	1135
		5	2.5	13.73	16.17	1.6	360	1145
			5	16.85	15.75	1.2	360	1135
			10	34.55	15.22	.70	36	1127
			15	35.62	15.84	.50	360	1117
			20	36.01	16.02	.35	360	1107
			25	36.16	15.94	.30	360	1058
			30	36.07	15.97	.35	15	1050
Pt. Spencer Station 3	3/10	1	2.5	26.84	16.62	1.0	NNE	1423
			5	26.86	16.58	.8	015	
			10	28.4	16.36			1403
			15	33.61	15.21			1410
			20	34.24	15.21			

89

Station	Date	Profile	Depth	Salinity	Temperature	Current Speed	Direction	Time
			25	34.59	15.21	.3	070	1447
			27.5	34.67	15.19	.24	036	1451
		2	2.5	26.0	16.81	1.1	NE	1512
			5	26.19	16.81	.8	NE	1520
			10	31.53	16.21	.7	E	1554
			15	34.45	15.46	.33	90	-1604
			20			.33	70	
			25	34.43	15.07	.2	ENE	1614
		3	2.5	28.97	16.73	.75	SE	1638
			5	27.62	16.60	.7	ESE	1653
			10	29.54	16.67	.9	72	1708
			15	33.56	15.84	.4	108	1721
			20	34.25	15.35	.35	108	1734
			25	35.10	15.26	.25	56	1745
			27	34.09	15.35	.15		1751
		4	2.5	21.5	16.26	.7	S	1837
			5	27.75	16.40	.5	SE	1847
			10	31.45	16.12	.65	SW	1852
			15	31.02	16.04	.5	SW	1914
			20	32.73	16.04	.1	E	1924
		5	5	24.23	16.38	.36	SW	2037
			10	31.46	16.12	.84	SW	2104
			15	31.09	16.38	.40	W	2120
			20	33.58	15.75	.10	NW	2124
			25	35.00	15.48	.20	NW	2140
		6	5	26.9	15.8	.72	W	2150
			10	30.71	16.21	.64	WNW	2202
			15	33.01	15.57	.47	NW	2210
			20	34.05	15.34	.38	NW	2220
			25	34.45	15.10	.5	NW	2240

69

Station	Date	Profile	Depth	Salinity	Temperature	Current Speed	Direction	Time
		7	5	26.00	16.43	.64	NW	2243
			10	30.19	15.85	.68	Nw	2248
			15	33.48	15.82	.72	NW	2314
			20	34.10	15.43	.40	NW	2315
			25	35.0	15.57	.24	NW	2321
	3/11	8	5	26.91	16.07	.8	NW	0000
			10	33.27	16.55	.6	NW	0006
			15	33.90	15.11	.6	NW	0015
			20	35.0	15.0	.6	NW	0030
			25	35.27	16.25	.56	NW	0040
		9	5	27.89	16.39			0045
			10	33.04	15.25	.6	NW	
			15			1.0	NW	
			20			.4	NW	0153
		10	5	29.14	16.34	.8	NW	0212
			10	34.50	15.29	.8	NW	0220
			15	34.65	15.28	.8	W	0225
			20	35.00	15.35	.8	WNW	0230
			25	35.35	15.32	.45	W	0250
		11	5	28.85	16.10	.8	NW	0312
			10	34.5	15.11	1.0	NW	0320
			15	34.56	15.25	.8	NW	0330
			20	34.70	15.05	.75	NW	0335
Reliance	3/8	1	5	33.87	15.10	.42	270	2337
			10	33.90	15.05	.40	270	2332
			15	33.92	15.05	.35	270	2328
			25	33.97	15.06	.25	252	2325
			45	33.97	15.10	.20	216	2310

70

Station	Date	Profile	Depth	Salinity	Temperature	Current Speed	Direction	Time
	3/9	2	5	33.90	14.90	.40	270	0003
			10	33.89	15.01	.35	270	0009
			15	33.96	15.00	.30	270	0018
			25	33.95	14.95	.20	252	0030
			35	33.96	14.92	.30	234	0036
			44	33.71	15.00	.25	360	0043
		3	5	33.96	14.88	.20	234	0115
			10	33.88	15.00	.30	340	0124
			15	33.60	15.02	.25	360	0130
			25	33.61	14.81	.20	324	0142
			35	34.05	14.89	.25	234	0152
			44	36.24	14.93	.25	270	0157
		4	5	36.43	14.93	.15	234	0205
			10	33.67	14.78	.20	234	0209
			15	33.70	14.80	.15	234	0215
			25	34.16	14.86	.15	252	0225
			35	34.03	14.90	.15	270	0232
			44	34.42	14.85	.25	270	0239
		5	5	34.45	14.84	.15	360	0247
			10	34.40	14.85	.20	360	0255
			15	34.30	14.84	.20	360	0315
			25	34.53	14.79	.15	360	0325
			35	34.35	14.80	.20	360	0333
			44	34.35	14.85	.15	360	0341
		6	5	34.70	14.75	.15	360	0347
			10	34.56	14.80	.20	360	0357
			15	34.53	14.80	.15	360	0405
			25	34.35	14.73	.15	270	0410
			35	34.10	14.66	.10	360	0419
			44	34.51	14.72	.05	252	0428

71

Station	Date	Profile	Depth	Salinity	Temperature	Current Speed	Direction	Time
		8	5	34.05	14.72	.08	360	0600
			10	34.03	14.80	.10	360	0610
			15	34.02	14.82	.05	360	0622
			25	34.11	14.73	0.0	180	0643
			35	34.0	14.79	0.0	360	0706
			44	34.05	14.85	.20	328	0718
		9	5	3?.86	14.82	0.0	72	0842
			10	33.95	14.66	0.0	360	0821
			15	33.74	14.70	0.05	360	0812
			25	33.92	14.75	0.0	360	0804
			35	33.85	14.72	0.0	342	0755
			44	34.14	14.82	.25	342	0735
Pt. Estero Station A	3/16	1	2	27.33	14.77		115	2153
			5	27.48	14.57	.38	115	
			10	27.67	14.59	.34	115	
			15	27.50	14.67	.25	130	
		2	2	25.45	14.25	.18	70	2329
			5	25.68	14.56	.24	90	
			10	27.15	14.38	.22	140	
			15	27.28	14.43	.43	180	
	3/17	3	2	21.75	13.92	.17	30	0054
			5	21.75	13.90	.12	70	
			10	23.40	14.15	.58	110	
			15	23.68	14.33	.56	105	
		4	2	22.95	13.93	.27	90	0220
			5	22.90	13.90	.33	90	
			10	23.68	13.95	.65	100	
			15	2?.48	14.11	.80	155	

Station	Date	Profile	Depth	Salinity	Temperature	Current Speed	Direction	Time
		5	2	21.86	13.54	.15	110	0345
			5	20.97	13.72	.25	120	
			10	24.96	14.05	.62	110	
			15	25.23	13.90	.74	110	
		6	2	22.19	13.52	.23	140	0514
			5	21.69	13.60	.26	100	
			10	22.78	13.80	.55	110	
			15	24.73	13.91	.75	105	
		7	2	21.28	13.65	.20	130	0645
			5	21.74	13.60	.29	120	
			10	22.90	13.76	.50	130	
			15	25.38	14.02	.57	130	
		8	2	31.24	13.68	.18	90	0815
			5	21.60	13.70	.14	90	
			10	21.60	13.70	.27	140	
			15	24.78	14.02	.34	140	
		9	2	24.64	14.00	.40	360	1000
			5	22.83	14.03	.50	300	
			10	22.82	14.07	.65	280	
			15	23.86	14.16	.45	280	
		10	2	23.78	14.16	.70	340	1130
			5	24.75	14.20	.80	340	
			10	23.95	14.20	.38	340	
			15	23.95	14.28	.36	270	
		11	2	24.00	14.20	.52	360	1255
			5	22.30	14.00	.55	350	

73

Station	Date	Profile	Depth	Salinity	Temperature	Current Speed	Direction	Time
			10	22.20	13.90	37	330	
			15	22.12	13.91	.46	340	
		12	2	21.46	14.20	.37		1450
			5	21.46	13.97	.46	360	
			10	21.42	13.80	.32	340	
			15	22.36	13.87		340	
		13	2	20.70	14.21	.26	300	2057
			5	20.54	14.20	.58	290	
			10	27.45	14.66	.33	330	
			15	27.30	14.67	.19	360	
		14	2	17.30	13.85	.22	280	2210
			5	22.85	14.10	.34	250	
			10	23.45	14.52	.24	330	
			15	29.00	14.62	.12	330	
		15	2	09.30	13.80	.10	110	2320
			5	19.80	14.15	.25	180	
			10	26.70	14.55	.10	300	
			15	28.23	14.76	.10	90	
	3/18	16	2	13.80	13.20	.28	90	0024
			5	18.32	13.95	.36	160	
			10	27.95	14.74	.26	120	
			15	27.90	14.75	.38	120	
		17	2	18.53	14.20	.58	110	0132
			5	20.89	14.32	.44	130	
			10	25.95	14.60	.52	120	
			15	27.55	14.60	.51	90	

74

Station	Date	Profile	Depth	Salinity	Temperature	Current Speed	Direction	Time
		18	2	19.84	14.42	.78	90	0237
			5	21.35	14.20	.68	120	
			10	26.78	14.37	.76	120	
			15	26.43	14.25	.47	105	
		19	2	21.08	14.18	.93	100	0350
			5	21.45	14.22	.86	95	
			10	24.60	14.45	.68	120	
			15	26.36	14.23	.45	95	
		20	2	21.54	14.17	.90	90	0522
			5	22.49	14.08	.80	110	
			10	22.75	14.00	.65	125	
			15	26.12	14.33	.38	90	
		21	2	21.80	14.21	.77	120	0655
			5	22.38	14.13	.63	110	
			10	23.34	14.11	.43	140	
			15	26.25	14.19	.20	60	
		22	2	21.52	14.18	.45	105	0751
			5	22.37	14.13	.28	105	
			10	25.12	14.07	.12	175	
			15	25.96	14.16	.06	205	
		23	2	21.94	14.35	.27	110	0920
			5	22.35	14.24	.00	185	
			10	23.52	14.28	.17	235	
			15			.16	260	
		24	2	21.45	14.35	.27	160	1007
			5	22.93	14.33	.43	180	
			10	20.25	14.41	.23	250	
			15	21.40	14.46	.18	280	

75

Station	Date	Profile	Depth	Salinity	Temperature	Current Speed	Direction	Time
		25	2	2.05	15.55	.17	250	1110
			5	22.63	14.55	.33	220	
			10	17.96	14.51	.36	270	
			15	26.40	14.55	.30	280	
		26	2	6.50	16.76	.28	240	1225
			5	22.40	14.70	.40	250	
			10	22.90	14.50	.32	270	
			15	25.85	14.55	.33	260	
Pt. Estero Station B	3/15	1	5	27.70	14.01	.60	230	
			10	28.70	14.56	.52	225	
			15	29.77	14.27	.63	225	
			20	29.98	14.08	.74	225	
			25	31.48	14.80	.35	216	2300
		2	5	27.45	13.63	.77	125	
			10	27.50	13.54	.63	135	
			15	29.96	14.59		135	
			20	29.46	14.61	.76	135	
	3/16		25	29.70	14.66	.44	145	0005
		3	5	28.07	13.61	.93	130	
			10	28.10	13.57	.87	140	
			15	28.26	13.86	.78	135	
			20	29.33	14.45	.45	130	
			25	30.71	14.84	.16	100	0120
		4	5	28.18	13.73	.86	100	
			10	28.45	13.83	.81	105	
			15	28.85	14.05	.42	112	
			20	29.95	14.50	.34	115	
			25	30.09	14.33	.00	135	0232

Station	Date	Profile	Depth	Salinity	Temperature	Current Speed	Direction	Time
		5	5	28.75	13.77	.72	102	
			10	28.75	13.74	.63	105	
			15	29.42	14.15	.33	118	
			20	29.89	14.25	.04	110	
			25	29.92	14.35	.10	73	0355
		6	5	26.60	13.61	.43	75	
			10	28.98	13.65	.37	75	
			15	29.01	13.77	.34	275	
			20	29.45	14.19	.36	100	
			25	30.12	14.55	.26	345	0518
		7	5	29.28	13.59	.49	280	
			10	29.32	13.52	.45	255	
			15	29.24	13.55	.20	345	
			20	30.22	14.50	.33	30	
			25	31.92	15.04	.15	65	0650
		8	5	29.33	13.52	.36	0	
			10	29.27	13.73	.34	0	
			15	29.65	13.72	.30	15	
			20	32.47	14.89	.45	10	
			25	33.30	15.20	.42	20	0805
		9	5	29.49	13.87	.35	15	
			10	30.17	14.54	.60	25	
			15	33.98	15.26	.48	20	
			20	34.03	14.39	.46	15	
			25	34.21	15.37	.34	15	0840
		10	5	30.40	14.23	.36	0	
			10	31.92	14.58	.77	0	
			15	33.87	15.14	.63	0	
			20	33.76	15.17	.35	0	
			25	33.69	15.18	.21	0	1110

77

Station	Date	Profile	Depth	Salinity	Temperature	Current Speed	Direction	Time
		11	5	30.51	14.23	.53	0	
			10	31.24	14.47	.63	0	1145
Pt. Estero Station C	3/20	1	2	16.45	14.25	.58	90	
			5	28.53	15.22	.31	80	
			10	33.52	15.15	.12	60	
			15	33.90	15.46	.13	280	0156
		2	2	9.60	13.86	2.2	110	
			5	29.60	15.05	.56	100	
			10	33.45	15.05	.23	100	
			15	34.08	15.20	.06	160	0300
		3	2	15.50	15.94	2.2	120	
			5	29.18	15.25	.64	110	
			10	32.57	14.90	.25	110	
			15	33.85	15.49	.07	130	0400
		4	2	15.45	17.40	1.75	130	
			5	31.20	15.18	.63	130	
			10	33.20	15.23	.20	120	
			15	34.40	15.73	.04	120	0454
		5	2	18.52	16.75	.80	120	
			5	26.00	15.75	.58	130	
			10	33.62	15.51	.16	140	
			15	33.55	15.56	.03	150	0550
		6	2	17.46	16.23	.77	110	
			5			.42	126	
			10	32.73	15.18	.18	126	
			15	33.72	15.30	.23	320	0640
		7	2	21.25	15.45	.60	115	
			5	27.70	15.64	.37	150	
			10	31.70	15.20	.14	345	
			15	33.48	15.42	.38	345	
			17.5	33.54	15.22	.42	345	0826

78

Station	Date	Profile	Depth	Salinity	Temperature	Current Speed	Direction	Time
		8	2	21.15	15.44	.38	170	
			5	21.50	15.85	.50	190	
			10	31.01	15.35	.02	325	
			15	33.04	15.08	.26	330	
			17.5	33.23	15.29	.36	340	1000
Pt. Estero Station D	3/18	1	5	27.45	15.35	.25	40	
			10	29.68	15.00	.33	340	
			15	31.30	15.11	.30	50	2059
		2	5	27.45	15.35	.25	40	
			10	29.55	15.19	.37	50	
			25	30.85	15.05	.41	90	2220
		3	5	27.75	15.35	.25	90	
			10	29.50	15.18	.43	180	
			25	28.70	15.60	.36	180	2334
	3/19	4	2	24.80	15.21	.10	45	
			5	24.70	15.65	.00	55	
			10	27.23	15.35	.38	190	
			25	31.75	14.83	.36	200	0140
		5	2	23.40	16.10	.45	110	
			5	23.58	15.26	.50	145	
			10	27.72	15.16	1.00	150	
			25	31.58	14.94	.40	180	0314
		6	2	17.70	15.46	.57	90	
			5	23.86	15.22	.78	125	
			10	30.78	14.76	.82	165	
			25	31.58	14.85	1.00	165	0500

79

Station	Date	Profile	Depth	Salinity	Temperature	Current Speed	Direction	Time
		7	2	22.03	15.18	.05	160	
			5	26.91	15.18	.65	170	
			10	30.71	15.02	.65	185	
			25	31.17	15.08	.38	200	0647
		8	2	16.76	15.25	.26	200	
			5	26.61	15.11	.63	210	
			10	29.86	14.96	.57	250	
			25	30.45	15.07	.32	260	0730
Dependable	3/15	1	2.5	22.54	13.49	1.50	70	2115
			5	36.15	16.45	0.30	80	2120
			10	36.53	15.85	0.15	100	2125
			15	36.61	15.84	0.18	110	2130
			25	36.28	15.77	0.10	80	2135
			35	36.94	15.84			2142
			45	37.06	15.72			2150
		2	2.5	21.80	13.45			2218
			5	35.81	16.38	0.06	80	2220
			10	36.06	16.18	0.25	95	2227
			15	36.11	15.90	0.17	125	2231
			25	36.32	15.80	0.18	160	2237
			35	36.34	15.78	0.13	170	2240
			45	36.44	15.76			2245
		3	2.5	22.42	13.89	0.25	90	2247
			5	34.00	15.28	0.20	90	2350
	3/16		10	36.00	16.46	0.34	110	0000
			15	36.18	15.91	0.22	120	0006
			25	36.44	15.77	0.18	125	0013
			35	36.48	15.84	0.14	110	0018
			45	36.48	15.76	0.08	110	0023

80

Station	Date	Profile	Depth	Salinity	Temperature	Current Speed	Direction	Time
		4	2.5	21.54	13.93		110	0040
			5	31.46	15.42	0.38	110	0045
			10	35.94	16.53	0.24	120	0052
			15	36.17	15.93	0.15	130	0057
			25	36.41	15.84	0.00	100	0105
			35	36.50	15.82	0.07	180	0109
			45	36.71	15.83	0.00	120	0115
		5	2.5	24.15	14.12	1.0	130	0140
			5	26.84	15.16	0.55	120	0146
			10	36.17	16.79	0.3	130	0152
			15	36.47	16.12	0.15	150	0158
			25	36.29	15.91	0.15	90	0204
			35	36.51	15.90	0.12	90	0210
			45	36.54	15.79	0.0	100	0216
		6	2.5	28.8	15.4	0.58	130	0240
			5	30.12	15.48	0.58	130	0250
			10	32.23	15.83	0.05	150	0256
			15	36.22	16.68	0.0	160	0302
			25	36.31	15.82	0.0	110	0308
			35	36.30	15.85	0.0	100	0314
			45	36.45	15.85	0.0	85	0320
		7	2.5	26.54	15.15	0.85	120	0335
			5	29.83	15.77	0.75	130	0341
			10	32.32	16.16	0.34	100	0345
			15	33.16	16.55	0.28	45	0351
			25	36.30	16.00	0.15	15	0357
			35	36.40	15.9	0.28	30	0403
			45	36.31	15.9	0.22	35	0410

Station	Date	Profile	Depth	Salinity	Temperature	Current Speed	Direction	Time
		8	2.5	error		0.58	140	0440
			5	31.62	16.14	0.64	150	0450
			10	33.23	16.34	0.25	150	0458
			15	34.68	16.38	0.22	130	0504
			25	36.36	15.94	0.20	45	0510
			35	36.50	15.84	0.21	45	0520
			45	36.56	15.76	0.17	50	0528
		9	2.5	29.28	14.69	0.62	160	0541
			5	31.91	16.34	0.70	200	0600
			10	33.79	16.58	0.35	90	0608
			15	36.31	16.64	0.35	90	0618
			25	37.60	15.92	0.25	55	0628
			35	36.96	16.01	0.25	55	0636
			45	36.77	15.89	0.30	65	0645
		10	2.5	26.09	14.08	0.70	190	07C0
			5	34.76	16.30	0.15	200	0712
			10	35.06	16.51	0.10	110	0725
			15	36.21	16.31	0.16	80	0733
			25	36.58	15.92			0745
			35	36.50	15.90	0.15	72	0750
			45	36.62	15.89	0.15	75	0800
		11	2.5	28.23	15.08	1.20	290	0900
			5	32.47	15.96	0.60	270	0908
			10	32.62	15.94	0.20	180	0916
			15					
		12	2.5	30.11	15.14	1.40	360	1016
			5	28.83	15.18	1.45	360	1019
			10	29.03	15.87	1.40	360	1030
			15	35.63	16.31	0.20	270	1040
			25	36.80	16.13	0.38	180	1050
			35	37.16	16.00	0.35	180	1100
			45	37.15	16.11	0.20	180	1110

Station	Date	Profile	Depth	Salinity	Temperature	Current Speed	Direction	Time
		13	2.5	29.65	15.70	1.00	360	1133
			5	28.84	15.58	1.00	360	1143
			10	30.81	15.60	0.60	335	1154
			15	34.03	15.77	0.35	255	1203
			25	37.31	16.01	0.60	216	1212
			35	37.17	15.96	0.50	200	1216
			45	37.14	15.97	0.45	185	1225
		14	2.5	25.3	14.9	1.3	360	1235
			5	25.85	14.9	1.15	360	1247
			10	27.8	15.0	0.4	345	1253
			15	35.4	15.8	0.45	245	1305
			25	38.0	16.1	0.9	220	1315
			35	38.8	16.0	0.6	225	1323
			45	37.4	16.0	0.6	200	1337
		15	2.5	14.07	14.00	1.3	20	1345
			5	14.78	14.13	1.2	30	1355
			10	34.7-35.3	15.0-16.2	0.5	270	1400
			15	37.82	15.92	0.46	240	1410
			25	36.71	16.21	0.70	200	1418
			35	37.15	16.13	0.60	200	1425
			45	37.05	16.08	0.55	190	1435
		16	2.5	11.94	13.88	1.30	355	1510
			5	12.08	13.77	1.30	360	1543
			10	34.80	16.12	1.3	360	1612
			15	33.30	15.58	1.4	360	1617
			25	36.60	16.14	1.3	340	1626
			35	36.50	16.22	1.4	20	1704
			45	36.49	16.14	1.0	340	1710

83

Station	Date	Profile	Depth	Salinity	Temperature	Current Speed	Direction	Time
		17	2.5	14.56	13.68	0.60	360	1720
			5	26.04	14.12	0.20	270	1742
			10	30.51	15.47	0.30	270	1755
			15	33.63	15.79	0.70	225	1805
			25	35.00	16.18	0.80	225	1810
			35	36.25	16.24	0.70	160	1825
			45	36.24	16.28	0.50	180	1845
		18	2.5	19.90	13.94			1910
			5	19.90	13.92	0.2	320	1930
			10	21.28	14.65	0.5	250	1958
			15	30.05	15.85	0.8ᶜ	250	2003
			25	35.73	16.19	0.70	200	2015
			35	35.70	16.25	0.64	180	2025
			45	35.76	16.22	0.60	160	2032
		19				0.2		
			5	20.82	14.10			2058
			10	28.88	15.42	0.4	270	2130
			15	31.08	16.08	1.0	250	2200
			25	32.00	16.20	1.1	225	2210
			35	35.14	16.16	1.0	180	2117
			45	35.20	16.25	0.7	180	2250
		20						
			5			0.1	270	2300
			10	26.00	15.83	0.7	220	2322
			15	27.78	15.89	0.8	205	2338
			25	34.40	15.35	0.6	198	2352
			35	34.35	15.92	1.1	200	2356
	3/17		45	34.58	15.92	0.3	190	0006
		21	2.5					
			5	24.80	15.1	0.7	320	0040
			10	27.6	15.5	0.5	350	0050
			15	24.0	15.04	0.6	230	0105
			25	31.8	16.07	0.8	220	0120
			35			1.0	200	0200
			45	38.7	15.66	1.2	110	0230

84

Station	Date	Profile	Depth	Salinity	Temperature	Current Speed	Direction	Time
		22						
			5	25.4	15.04	0.6	360	0255
			10	26.2	15.52	0.5	285	0313
			15	27.2	15.30	1.2	200	0332
			25	32.92	15.80	0.9	190	0350
			35	33.26	15.63	1.0	185	0410
			45	33.70	15.60	0.8	185	0420
		23						
			5	25.9	14.90	0.8	345	0500
			10	25.92	14.95	0.5	345	0515
			15	26.3	14.97	0.8	285	0525
			25	32.88	15.76	0.7	160	0535
			35	33.05	15.72	0.8	200	0545
			45	33.34	15.61	0.6	210	0555
		24						
			5	25.87	14.70	0.5	360	0630
			10	28.07	15.13	0.5	340	0638
			15	27.5	15.56	0.8	260	0645
			25	33.00	15.68	0.7	210	0655
			35	33.08	15.61	0.7	200	0702
			45	33.68	15.64	0.6	200	0712
		25						
			5	26.58	14.95	0.40	10	0745
			10	26.79	15.07	0.40	290	0810
			15	28.42	15.12	0.30	10	0823
			25	32.54	16.00	0.50	250	
		26						
			5	28.89	15.55	0.40	320	0957
			10	27.27	15.28	0.70	350	1011
			15	27.88	15.45	0.70	280	1034
			25	31.50	15.89	0.60	265	1043
			35	33.98	15.74	0.80	260	1055
			45	34.46	15.98	0.60	265	1107

Station	Date	Profile	Depth	Salinity	Temperature	Current Speed	Direction	Time
		27						
			5			0.6	80	
			10	27.60	15.62	0.6	340	1124
			15	28.89	15.58	0.8	265	1132
			25	32.95	15.77			1138
			35	34.10	15.97	0.7	280	1154
			45	34.68	16.28	0.5	280	1201
		28						
			10	29.41	15.65	0.50	30	1210
			15	29.15	15.66	0.25	330	1222
			25	32.91	15.84	0.80	270	1232
			35	34.85	16.0	0.65	285	1241
			45	34.85	16.08	0.40	290	1248
		29	10	28.83	15.60	0.6	70	1300
			15	30.20	15.62	0.15	60	1307
			25	29.48	16.0	0.43	310	1318
			35	35.12	16.22	0.40	320	1330
			45	35.00	16.24	0.65	310	1340
		30	10	28.45	15.81	0.8	85	1345
			15	29.36	15.76	0.4	105	1355
			25	32.42	15.89	0.65	270	1403
			35	35.14	16.26	0.4	306	1409
			45	35.17	16.22	0.4	340	1419
		31	10	28.64	15.77	0.40	90	1429
			15	29.45	15.62	0.15	65	1442
			25	35.0	15.92	0.68	300	1452
			35	35.45	16.28	0.52	345	1500
			45	35.41	16.15	0.45	350	1510
		32	5	29.04	15.86	0.65	95	1522
			10	29.45	15.66	0.10	85	1532
			15	31.45	15.76	0.18	45	1542
			25	35.85	16.14	0.55	345	1554

98

Station	Date	Profile	Depth	Salinity	Temperature	Current Speed	Direction	Time
			35	35.89	16.18	0.40	306	1610
			45	35.73	16.30	0 40	324	1617
		33	5	29.15	15.92	0.70	90	1622
			10	29.28	15.77	0.30	90	1630
			15	31.45	15.92	0.55	270	1658
			25	35.55	16.26	0.38	345	1708
			35	35.44	16.24	0.35	345	1717
			45	35.66	16.21	0.42	345	1727
		34	5	29.25	15.91	0.35	95	1818
			10	29.55	15.82	0.10	90	1822
			15	31.71	15.92	0.32	250	1829
			25	35.12	16.29	0.30	320	1837
			35	35.55	16.30	0.25	350	1852
			45	35.91	16.26	0.30	360	1902
		35	5	29.24	16.05	0.30	225	1911
			10	31.76	15.92	0.30	288	1919
			15	33.00	16.24	0.10	306	1923
			25	35.88	16.32	0.10	342	1937
			35	35.82	16.40	0.25	N	1947
			45	36.10	16.25	0.30	350	1955
		36	5	32.42	16.99	0.5	195	2005
			10	34.0	16.24	0.45	170	2018
			15	33.66	16.15	0.42	180	2027
			25	35.81	16.25	0.10	270	2036
			35	35.72	16.33	0.3	0	2045
			45	36.05	16.11	0.33	40	2055
		37	5	33.03	16.14	0.32	170	2105
			10	33.08	16.26	0.62	170	2115
			15	33.58	16.25	0.48	185	2124
			25	34.12	16.18	0.36	100	2148
			35	36.08	16.24	0.34	75	2200
			45	36.28	16.17	0.28	360	2210

Station	Date	Profile	Depth	Salinity	Temperature	Current Speed	Direction	Time
		38	5	33.66	16.18	0.38	175	2218
			10	33.45	16.25	0.45	165	2228
			15	35.05	16.18	0.58	165	2236
			25	35.65	16.28	0.38	175	2247
			35	36.05	16.32	0.32	105	2254
			45	36.62	16.16	0.25	75	2303
		39	5	33.25	16.10	0.78	170	2311
			10	33.75	16.24	0.65	165	2322
			15	34.34	16.28	0.65	165	2329
			25	35.64	16.32	0.50	105	2340
			35	36.24	16.27	0.50	110	2350
			45	36.71	16.18	0.48	100	2359
	3/18	40	5	32.62	15.92	0.65	180	0013
			10	33.81	16.05	0.70	140	0022
			15	32.59	16.17	0.50	160	0029
			25	35.41	16.12	0.60	110	0038
			35	36.41	16.28	0.60	100	0047
			45	36.50	16.19	0.55	100	0055
		41	5	33.47	16.09	0.85	170	0112
			10	32.70	16.07	0.80	150	0125
			15	33.89	16.05	0.70	180	0133
			25	35.37	16.29	0.55	180	0141
			35	36.37	16.27	0.50	120	0151
			45	36.29	16.16	0.60	110	0200
		42	5	31.62	15.81	0.90	140	0218
			10	33.03	16.00	0.80	150	0250
			15	32.13	15.91	0.80	160	0258
			25	34.75	16.17	0.65	200	0307
			35	36.02	16.24	0.55	160	0317
			45	36.10	16.18	0.45	150	0326

88

Station	Date	Profile	Depth	Salinity	Temperature	Current Speed	Direction	Time
		43	5	28.93	15.57	0.68	120	0345
			10	29.11	15.62	0.70	140	0352
			15	32.64	15.93	0.95	210	0400
			25	34.31	16.98	0.65	230	0407
			35	35.64	16.28	0.50	170	0414
			45	35.70	16.12	0.65	165	0423
		44	5	28.53	15.46	0.85	120	0434
			10	29.20	15.61	0.75	150	0441
			15	30.30	15.92	0.80	220	0447
			25	34.29	16.07	0.70	230	0454
			35	35.10	16.23	0.50	180	0500
			45	35.29	16.06	0.65	170	0507
		45	5	26.53	15.40	0.75	130	0536
			10	29.51	15.62	0.70	160	0543
			15	32.81	15.73	1.50	200	0550
			25	34.12	15.90	0.70	220	0600
			35	34.78	16.17	0.60	210	0608
			45	35.27	16.16	0.45	200	0615
		46	5	28.96	15.55	0.75	150	0634
			10	31.98	15.74	0.85	170	0641
			15	33.76	15.75	0.80	210	0649
			25	34.15	16.00	0.70	234	0654
			35	35.16	16.04	0.65	207	0709
			45	35.33	16.20	0.65	180	0717
		47	5	29.94	15.72	0.90	160	0726
			10	31.12	15.73	0.90	180	0733
			15	33.82	15.73	0.85	200	0740
			25	34.20	15.75	0.70	220	0748
			35	34.55	15.97	0.70	200	0800
			45			0.65	180	0808

69

Station	Date	Profile	Depth	Salinity	Temperature	Current Speed	Direction	Time
		48	5	29.75	15.78	0.92	170	0821
			10	31.55	15.78	0.95	170	0835
			15	33.90	15.90	0.88	200	0840
			25	34.40	15.98	0.65	192	0847
			35	34.88	16.00	0.72	200	0855
			45	35.34	16.24	0.75	180	0914
		49	5	30.56	15.68	0.85	180	0920
			10	31.65	15.78	1.50	180	0934
			15	33.92	15.82	1.40	200	0946
			25	34.58	15.84	0.55	220	0948
			35	35.23	15.92	0.65	200	0957
			45	35.45	16.00	0.75	180	1005
		50	5	31.73	15.82	0.75	180	1025
			10	33.19	15.81	0.85	180	1032
			15	34.71	15.73	0.75	200	1040
			25	35.10	15.83	0.55	200	1053
			35	35.25	15.86	0.65	190	1102
			45	35.58	15.93	0.75	200	1113
		51	5	31.85	15.82	0.75	180	1130
			10	32.09	15.66	0.85	190	1150
			15	34.56	15.79	0.60	200	1154
			25	34.55	16.00	0.45	234	1200
			35	34.64	15.72	0.55	216	1210
			45	35.12	15.81	0.65	198	1214
		52	5	31.81	15.89	0.75	180	1222
			10	34.19	15.79	0.65	180	1233
			15	34.94	15.72	0.50	200	1251
			25	35.99	15.75	0.40	220	1255
			35	35.01	15.68	0.60	230	1304
			45	35.0	15.70	0.70	200	1312

Station	Date	Profile	Depth	Salinity	Temperature	Current Speed	Direction	Time
		53	5	32.12	15.61	0.75	190	1318
			10	34.15	15.65	0.55	200	1327
			15	34.64	16.06	0.50	200	1332
			25	34.44	15.96	0.40	224	1342
			35	34.70	15.75	0.55	220	1355
			45	34.78	15.78	0.70	198	1405
		54	5	34.15	15.80	0.60	200	1425
			10	34.55	15.80	0.55	200	1438
			15	34.42	15.78	0.40	216	1500
			25	34.23	15.76	0.40	234	1514
			35	34.37	15.61	0.40	180	1532
			45	34.55	15.62	0.60	198	1542
		55	5	34.26	15.87	0.45	216	1548
			10	34.38	15.79	0.40	210	1605
			15	33.96	15.80	0.35	200	1608
			25	34.20	15.82	0.30	216	1620
			35	34.52	15.74	0.55	216	1630
			45	34.75	15.61	0.65	207	1628
		56	5	33.47	16.07	0.50	198	1643
			10	34.12	15.84	0.45	216	1703
			15	33.94	15.77	0.30	225	1707
			25	34.25	15.70	0.30	210	1719
			35	34.35	15.58	0.50	195	1721
			45	34.4	15.53	0.55	195	1735
		57	5	33.34	16.1	0.30	155	1744
			10	34.01	15.70	0.50	265	1753
			15	34.14	15.83	0.35	190	1807
			25	34.22	15.75	0.45	190	1817
			35	34.41	15.54	0.50	200	1825
			45	34.46	15.5	0.55	200	1833

T6

Station	Date	Profile	Depth	Salinity	Temperature	Current Speed	Direction	Time
		58	5	33.62	16.12	0.50	270	1842
			10	33.84	16.15	0.45	234	1845
			15	35.50	15.82	0.30	216	1852
			25	34.51	15.72	0.35	198	1858
			35	34.42	15.48	0.40	225	1905
			45	34.50	15.54	0.60	198	1917
		59	5	33.95	16.24	0.45	252	1924
			10	34.14	16.02	0.40	225	1936
			15	34.05	15.86	0.35	216	1945
			25	34.16	15.72	0.40	198	1954
			35	34.62	15.56	0.50	198	2001
			45	34.42	15.58	0.55	198	2007
		60	5	33.93	16.05	0.20	270	2014
			10	33.96	16.06	0.30	234	2024
			15	36.69	15.97	0.25	216	2031
			25	34.40	15.78	0.45	189	2039
			35	34.48	15.58	0.50	198	2047
			45	34.94	15.50	0.55	198	2055
		61	5	34.49	16.09	0.10	288	2106
			10	34.66	15.97	0.15	220	2114
			15	36.77	16.98	0.30	216	2120
			25	33.53	15.70	0.55	180	2140
			35	33.57	15.75	0.50	180	2148
			45	33.70	15.65	0.55	198	2154
		62	5	33.42	15.99	0.10	342	2200
			10	33.50	16.03	0.20	188	2218
			15	33.46	15.97	0.30	198	2228
			25	33.49	15.94	0.45	180	2236
			35	33.87	15.57	0.65	180	2246
			45	33.92	15.48	0.70	190	2254

Station	Date	Profile	Depth	Salinity	Temperature	Current Speed	Direction	Time
		63	5	33.94	15.99	0.05	324	2304
			10	33.72	16.03	0.25	144	2313
			15	33.76	16.06	0.35	162	2324
			25	33.74	16.05	0.50	180	2334
			35	33.98	15.64	0.75	180	2344
			45	34.06	15.44	0.70	171	2357
	3/19	64	5	33.60	16.02	0.05	108	0010
			10	33.78	16.08	0.30	115	0022
			15	33.67	15.97	0.35	135	0030
			25	33.70	16.17	0.55	170	0042
			35	34.02	15.40	0.85	175	0054
			45	34.0	15.41	0.75	180	0105
		65	5	33.46	15.92	0.05	100	0112
			10	33.38	15.98	0.35	105	0172
			15	33.42	15.95	0.50	100	0131
			25	33.46	15.95	0.55	165	0141
			35	34.0	15.32	0.85	185	0150
			45	34.05	15.38	0.70	180	0200
		66	5	32.64	16.04	0.55	130	0212
			10	32.58	16.08	0.80	110	0221
			15	32.7	15.84	0.80	135	0231
			25	33.93	15.49	0.85	170	0241
			35	34.03	15.34	0.75	175	0250
			45	34.13	14.43	0.60	175	0300
		67	5	32.2	16.18	0.10	100	0312
			10	32.3	16.0	0.70	105	1323
			15	32.7	16.1	0.75	135	0331
			25	33.83	15.68	0.85	170	0340
			35	34.08	15.39	0.75	180	0347
			45	34.04	15.36	0.65	180	0357

Station	Date	Profile	Depth	Salinity	Temperature	Current Speed	Direction	Time
		68	5	32.3	16.31	0.10	80	0407
			10	32.9	16.11	1.50	115	0426
			15	31.73	16.24	1.10	140	0434
			25	33.2	16.01	1.40	185	0443
			35	34.08	15.64	1.50	205	0452
			45	34.26	15.40	0.84	210	0502
		69	5	28.65	16.72	0.90	100	0514
			10	29.78	16.56	0.75	135	0524
			15	31.58	16.50	0.65	170	0534
			25	32.84	16.23	0.90	185	0544
			35	34.11	15.92	0.85	220	0554
			45	34.28	15.56	0.70	280	0604
		70	5	28.76	16.67	1.90	100	0616
			10	31.92	16.30	1.10	135	0625
			15	32.44	16.27	0.75	175	0633
			25	34.21	15.94	0.70	205	0641
			35	34.30	16.00	0.65	230	0650
			45	34.32	15.86	0.45	235	0659
		71	5	30.88	16.62	0.75	110	0708
			10	32.04	16.30	0.70	155	0717
			15	32.47	16.24	0.65	160	0725
			25	34.14	16.05	0.55	210	0732
			35	34.36	16.0	0.55	220	0739
			45	34.45	15.8	0.35	220	0747
		72	5	30.43	16.61	0.75	135	0811
			10	32.70	16.02	0.65	170	0819
			15	33.68	15.94	0.45	188	0826
			25	34.65	16.19	0.35	235	0830
			35	34.71	15.82	0.35	235	0838
			45	34.68	15.89	0.35	235	0845

Station	Date	Profile	Depth	Salinity	Temperature	Current Speed	Direction	Time
		73	5	32.12	16.24	0.80	135	0850
			10	33.41	5.92	0.60	162	0905
			15	34.45	.15	0.30	180	0915
			25	34.74	.06	0.30	216	0920
			35	35.02	15.78	0.30	234	0930
			45	35.12	15.84	0.35	235	0940
		74	5	31.80	16.51	0.65	120	0955
			10	33.05	15.99	0.40	160	1005
			15	35.49	16.37	0.35	180	1015
			25	36.12	15.81	0.45	210	1025
			35	35.53	15.84	0.35	250	1035
			45	35.65	15.85	0.25	250	1047
		75	5	33.37	16.45	0.65	150	1100
			10	35.05	16.18	0.30	162	1109
			15	35.84	16.39	0.25	198	1118
			25	36.44	16.17	0.40	225	1125
			35	36.67	15.90	0.45	216	1133
			45	36.06	15.76	0.35	180	1141
		76	5	33.45	16.98	0.10	234	1147
			10	34.86	16.44	0.30	234	1200
			15	36.10	16.39	0.40	270	1207
			25	36.02	16.30	0.45	250	1215
			35	35.68	15.90	0.30	198	1225
			45	35.65	15.80	0.35	200	1233
		77	5	28.84	18.00	0.25	234	1245
			10	34.62	16.56	0.25	250	1307
			15	35.15	16.52	0.30	270	1315
			25	36.42	16.10	0.35	270	1320
			35	35.65	15.90	0.35	270	1332
			45	35.58	15.92	0.35	252	1340

Station	Date	Profile	Depth	Salinity	Temperature	Current Speed	Direction	Time
		78	5	31.42	17.72	0.10	279	1350
			10	34.25	16.79	0.25	228	1405
			15	35.40	16.48	0.20	288	1413
			25	35.79	16.09	0.45	198	1455
			35	35.56	15.92	0.45	262	1505
			45	35.55	15.90	0.30	270	1512
		79	5	28.00	17.98	0.15	36	1557
			10	34.18	16.50	0.20	216	1610
			15	34.96	16.56	0.25	270	1615
			25	35.54	15.94	0.35	270	1624
			35	35.43	15.86	0.40	252	1637
			45	35.29	15.87	0.45	270	1645
		80	5	29.14	17.76	0.10	315	1700
			10	34.22	16.59	0.20	322	1708
			15	33.55	16.26	0.35	315	1717
			25	35.36	15.96	0.30	298	1725
			35	35.34	15.92	0.25	262	1733
			45	35.36	15.88	0.30	270	1740
		81	5	23.30	17.67	0.05	330	1837
			10	34.17	16.30	0.10	320	1845
			15	34.90	16.24	0.25	280	1856
			25	35.23	15.97	0.30	290	1904
			35	35.25	15.92	0.35	270	1912
			45	35.15	15.91	0.30	275	1920
		82	5	23.63	17.44	0.05	330	1935
			10	33.76	16.35	0.15	300	1944
			15	34.33	16.35	0.25	290	1952
			25	35.24	15.90	0.30	270	2000
			35	35.18	15.96	0.30	270	2010
			45	35.16	16.08	0.30	280	2019

Station	Date	Profile	Depth	Salinity	Temperature	Current Speed	Direction	Time
		83	5	24.30	17.28	0.05	340	2030
			10	34.93	16.37	0.15	270	2038
			15	34.90	16.45	0.15	270	2043
			25	35.30	15.90	0.25	255	2053
			35	35.20	15.90	0.25	270	2103
			45	35.23	15.95	0.20	260	2111
		84	5	24.08	17.40	0.10	360	2127
			10	34.28	16.38	0.05	70	2135
			15	34.66	16.32	0.15	270	2144
			25	34.80	16.08	0.30	210	2153
			35	35.20	15.88	0.3`	270	2201
			45	35.30	15.96	0.25	270	2210
		85	5	23.51	17.42	0.10	270	2223
			10	34.77	16.43	0.15	260	2232
			15	34.74	16.52	0.10	250	2239
			25	35.31	15.84	0.20	225	2246
			35	35.42	15.94	0.25	260	2253
			45	35.34	15.98	0.20	255	2300
		86	5	24.46	17.30	0.10	110	2315
			10	33.85	16.65	0.05	110	2323
			15	34.75	16.57	0.15	170	2330
			25	35.23	16.03	0.15	205	2338
			35	35.40	15.88	0.20	250	2350
			45	35.28	15.94	0.15	243	2357
	3/20	87	5	26.70	17.04	0.15	126	0000
			10	33.14	16.65	0.15	180	0010
			15	34.90	16.36	0.25	162	0020
			25	35.27	15.92	0.15	198	0030
			35	35.28	15.92	0.10	216	0040
			45	35.42	15.93	0.10	234	0050

97

Station	Date	Profile	Depth	Salinity	Temperature	Current Speed	Direction	Time
		88	5	32.47	16.93	0.25	118	0100
			10	32.41	16.81	0.20	154	0110
			15	34.73	16.52	0.20	154	0120
			25	35.18	15.88	0.25	180	0130
			35	35.24	15.90	0.15	198	0140
			45	35.39	15.97	0.25	198	0150
		89	5	31.82	16.94	0.30	180	0200
			10	33.34	17.03	0.20	144	0210
			15	34.78	16.45	0.25	144	0220
			25	35.09	15.90	0.20	180	0230
			35	35.30	15.93	0.15	216	0240
			45	35.32	15.93	0.10	208	0250
		90	5	32.08	16.80	0.40	130	0300
			10	33.50	16.85	0.25	134	0310
			15	34.62	16.64	0.25	134	0320
			25	35.14	15.98	0.30	162	0330
			35	35.22	15.86	0.15	198	0344
			45	35.24	15.90	0.05	206	0350
		91	5	30.56	16.76	0.25	116	0400
			10	32.05	16.96	0.20	180	0410
			15	34.60	16.79	0.15	180	0420
			25	35.40	16.00	0.15	180	0430
			35	35.40	16.00	0.15	235	0440
			45	35.64	15.99	0.05	355	0450
		92	5	27.92	16.62	0.95	108	0500
			10	29.24	16.52	0.55	144	0510
			15	33.26	16.98	0.20	198	0520
			25	35.36	15.92	0.10	198	0530
			35	35.52	15.92	0.05	180	0540
			45	35.55	15.96	0.05	244	0543

99

Station	Date	Profile	Depth	Salinity	Temperature	Current Speed	Direction	Time
		93	5	29.05	16.67	0.65	151	0615
			10	33.23	16.86	0.20	180	0623
			15	34.80	16.87	0.05	188	0630
			25	35.29	15.98	0.10	206	0640
			35	35.54	15.91	0.05	144	0650
			45	35.82	15.98	0.05	90	0655
		94	5	31.12	16.88	0.30	144	0700
			10	31.48	16.93	0.15	185	0720
			15	34.50	16.96	0.10	180	0730
			25	35.58	15.89	0.10	180	0740
			35	35.64	15.91	0.05	200	0750
			45	35.67	15.97	0.10	310	0800
		95	5	31.88	16.97	0.35	165	0810
			10	34.16	16.93	0.05	170	0820
			15	34.37	16.81	0.15	215	0835
			25	35.55	15.83	0.10	235	0845
			35	35.60	15.86	0.05	260	0855
			45	35.66	15.88	0.25	250	0905

REFERENCES

Abramowitz, M., and I. A. Stegun, 1965, Handbook of mathematical functions. New York (Dover Publications, Inc.).

Bowden, K. F., 1962, Measurements of turbulence near the sea bed in a tidal current. J. Geophys. Res., 67(8):3181.

Haltiner, G. J., and F. L. Martin, 1959, Dynamical and physical meteorology. New York (McGraw-Hill Book Co., Inc.), 470 pp.

Johnson, J. W., and H. C. Hwang, 1961, Mixing and dispersion by wind waves. Inst. Engineering Research Tech. Rept., Series 138, Issue 5, Univ. California, Berkeley.

Kalinske, A. A., and C. F. Pien, 1944, Eddy diffusion. Industrial and Engineering Chemistry, 36:220-223.

Marmer, H. A., 1932, Tides and tidal currents. In Physics of the earth, V. Oceanography, Bull. National Research Council, No. 85, pp. 229-309.

Masch, F. D., 1961, Mixing and dispersing action of wind waves. Inst. Engineering Research Tech. Rept., Series 138, Issue 6, Univ. California, Berkeley, 106 pp.

McNown, J., and P. N. Lin, 1952, Sediment concentration and fall velocity. Proc. Second Midwestern Conf. on Fluid Mechanics. Ohio State Univ.

Murray, S. P., 1969, Current meters in use at the Coastal Studies Institute. Coastal Studies Bulletin, Louisiana State Univ., No. 3, pp. 1-15.

Orlob, G. T., 1959, Eddy diffusion in homogeneous turbulence. J. Hydraulics Div. Am. Soc. Civil Engrs., 85(HY9):75-101.

Orton, R. B., 1964, The climate of Texas and the adjacent Gulf waters. U.S. Dept. Commerce, Weather Bureau, p. 112.

Pritchard, D. W., 1966, Comment on the paper "Small-scale horizontal diffusion near the coast," by N. Ito, M. Fukuda, and Y. Tanigawa. International Atomic Agency Symposium on the Disposal of Radioactive Wastes into Seas, Oceans, and Surface Waters, Vienna, p. 482.

Reid, R. O., 1957, Modification of the quadratic bottom-stress law for turbulent channel flow in the presence of surface wind stress. Corps of Engineers, Beach Erosion Board Tech. Memo. No. 93, 33 pp.

Roberts, O. F. T., 1923, Scattering of smoke in a turbulent atmosphere. Proc. Royal Society of London, Series A, 104:640-654.

100

Scruton, P. C., 1956, Oceanography of Mississippi Delta sedimentary environ-
ments. Bull., Am. Assoc. Petrol. Geologists, 40:2864-2952.

Sutton, O. G., 1953, Micrometeorology. New York (McGraw-Hill Book Co., Inc.),
333 pp.

Sverdrup, H. U., M. W. Johnson, and R. H. Fleming, 1942, The oceans, their
physics, chemistry, and general biology. New York (Prentice Hall),
1087 pp.

Taylor, G. I., 1921, Diffusion by continuous movements. Proc. London Math.
Society, 20:196-212.

_____, 1935, Statistical theory of turbulence, Parts I-IV. Proc. Royal Society
of London, Series A, 151:421-478.

U.S. Coast and Geodetic Survey, ESSA, 1970, Tide tables, high and low water
predictions, east coast, North and South America, including Greenland.
U.S. Government Printing Office, p. 239.

Weather Bureau, U.S. Dept. of Commerce, 1959, Climatological and oceanographic
atlas for mariners. Vol. 1, North Atlantic Ocean.

Wiegel, R. L., 1962, Wind waves and swell. Proc. 7th Conf. on Coastal
Engineering.

Yudine, M. I., 1959, Physical consideratt on heavy particle diffusion.
Advances in geophysics, atmospheric diffusion and air pollution, 6:
185-192.

DOCUMENT CONTROL DATA - R & D

(Security classification of title, body of abstract and indexing annotation must be entered when the overall report is classified)

1. ORIGINATING ACTIVITY (Corporate author)	2a. REPORT SECURITY CLASSIFICATION
Coastal Studies Institute Louisiana State University Baton Rouge, Louisiana 70803	UNCLASSIFIED 2b. GROUP

3. REPORT TITLE

Oceanographic Observations and Theoretical Analysis of Oil Slicks During The Chevron Spill, March 1970

4. DESCRIPTIVE NOTES (Type of report and inclusive dates)

Final Report (March 1970 - July 1970)

5. AUTHOR(S) (First name, middle initial, last name)

Stephen P. Murray, W. G. Smith, Choule J. Sonu

6. REPORT DATE	7a. TOTAL NO. OF PAGES	7b. NO. OF REFS
July 1970	110	23

8a. CONTRACT OR GRANT NO.	9a. ORIGINATOR'S REPORT NUMBER(S)
DOT-CG-03,592-A	NONE
b. PROJECT NO. 714104/A/006	
c.	9b. OTHER REPORT NO(S) (Any other numbers that may be assigned this report)
d.	714104/A/006-2

10. DISTRIBUTION STATEMENT

Availability Unlimited. Document may be released to the Clearinghouse for Federal Scientific and Technical Information, Springfield, Virginia 22151, for sale to the public.

11. SUPPLEMENTARY NOTES	12. SPONSORING MILITARY ACTIVITY
Key words: oil slick, oil spill, oil slick growth and movement	U. S. Coast Guard Department of Transportation Washington, D. C. 20591

13. ABSTRACT

Oceanographic observations near the Chevron spilling well off the Mississippi Delta in March 1970 revealed relative roles of various physical factors of the regional estuarine system in the behavior of oil slicks. Surface stress from the wind was most important, at speeds above 15 mph the slick orientation was generally determined by the wind direction. The wind also indirectly affected oil which was sunk by dispersant in the wind waves promoted mixing, which in turn affected the vertical stability, hence eventually the velocity profile. Wind setups and setdowns were correlated with downward and upward isopycnal movements, respectively. Both calculations and observations showed that tidal currents produced an L-shaped slick geometry when winds were below about 15 mph. The diurnal rotation of the tidal currents served to limit the excursion length of oil from the source, keeping it short of the nearest shore. The presence of fresh water from the Mississippi River in the surface layer and the consequent development of convergence lines often formed a natural barrier, preventing oil from encroaching upon the shore. Theoretical analysis using turbulent diffusion theory disclosed that the area and length of a steady-state oil slick increased with oil discharge but decreased with current speed and the lateral diffusion coefficient. Slick width increased with the rate of discharge and decreased with current speed but was independent of the diffusion coefficient. The width/length ratio of an oil slick, which was notably independent of current speed, was controlled only by the diffusion coefficient and the oil discharge. In order to be able to predict oil slick behavior, understanding of the interaction between these multiple factors is essential and, for that end, the use of a multiple-sensor array with auto-matic data transfer and processing capability is recommended. (U)

DD FORM NOV 65 **1473**